Calhoun: The NPS Institutional Archive

DSpace Repository

Theses and Dissertations | 1. Thesis and Dissertation Collection, all items

2014-06

Characterization of the vertical structure of tidal currents in the Mouth of the Columbia River and evaluation of the SELFE model

Oxendine, Joseph R.

Monterey, California. Naval Postgraduate School

http://hdl.handle.net/10945/42701

This publication is a work of the U.S. Government as defined in Title 17, United States Code, Section 101. Copyright protection is not available for this work in the United States.

Downloaded from NPS Archive: Calhoun

http://www.nps.edu/library

Calhoun is the Naval Postgraduate School's public access digital repository for research materials and institutional publications created by the NPS community. Calhoun is named for Professor of Mathematics Guy K. Calhoun, NPS's first appointed -- and published -- scholarly author.

Dudley Knox Library / Naval Postgraduate School
411 Dyer Road / 1 University Circle
Monterey, California USA 93943

NAVAL POSTGRADUATE SCHOOL

MONTEREY, CALIFORNIA

THESIS

CHARACTERIZATION OF THE VERTICAL STRUCTURE OF TIDAL CURRENTS IN THE MOUTH OF THE COLUMBIA RIVER AND EVALUATION OF THE SELFE MODEL

by

Joseph R. Oxendine

June 2014

Thesis Advisor: Thomas H. C. Herbers
Second Reader: Tim Janssen

Approved for public release; distribution is unlimited

THIS PAGE INTENTIONALLY LEFT BLANK

REPORT DOCUMENTATION PAGE

Form Approved OMB No. 0704-0188

Public reporting burden for this collection of information is estimated to average 1 hour per response, including the time for reviewing instruction, searching existing data sources, gathering and maintaining the data needed, and completing and reviewing the collection of information. Send comments regarding this burden estimate or any other aspect of this collection of information, including suggestions for reducing this burden, to Washington headquarters Services, Directorate for Information Operations and Reports, 1215 Jefferson Davis Highway, Suite 1204, Arlington, VA 22202-4302, and to the Office of Management and Budget, Paperwork Reduction Project (0704-0188) Washington DC 20503.

1. AGENCY USE ONLY *(Leave blank)*	**2. REPORT DATE** June 2014	**3. REPORT TYPE AND DATES COVERED** Master's Thesis

4. TITLE AND SUBTITLE
CHARACTERIZATION OF THE VERTICAL STRUCTURE OF TIDAL CURRENTS IN THE MOUTH OF THE COLUMBIA RIVER AND EVALUATION OF THE SELFE MODEL

5. FUNDING NUMBERS

6. AUTHOR(S) Joseph R. Oxendine

7. PERFORMING ORGANIZATION NAME(S) AND ADDRESS(ES)
Naval Postgraduate School
Monterey, CA 93943-5000

8. PERFORMING ORGANIZATION REPORT NUMBER

9. SPONSORING /MONITORING AGENCY NAME(S) AND ADDRESS(ES)
N/A

10. SPONSORING/MONITORING AGENCY REPORT NUMBER

11. SUPPLEMENTARY NOTES The views expressed in this thesis are those of the author and do not reflect the official policy or position of the Department of Defense or the U.S. Government. IRB Protocol number ____N/A____.

12a. DISTRIBUTION / AVAILABILITY STATEMENT
Approved for public release; distribution is unlimited

12b. DISTRIBUTION CODE

13. ABSTRACT (maximum 200 words)

Lack of measurements has led to a poor understanding of tidal currents within the Mouth of the Columbia River (MCR). Shipboard ADCP measurements are a technically viable means to measure these currents and their vertical structures. Shipboard ADCP measurements from a three-week long cruise conducted by the R/V Point Sur are used in this study. Transects along the main shipping channel and across the bar were extracted using criteria of constant speed and heading. Vertical sections from each transect were compared with predictions from the SELFE model in order to evaluate the models' ability to predict these currents.

Observed flood currents within the river are bottom intensified with slight river outflow at the surface early in the flood cycle. Complete reversal of the flow throughout the column is experienced later as the flood fully develops. Ebb currents are much stronger and more homogenous throughout the water column due to the combination of river outflow and tidal current.

Inside the river mouth, the SELFE model agrees qualitatively well with observations, with only a few discrepancies. Outside the river mouth, the SELFE model does not resolve the observed vertical structure, possibly due to coarse grid resolution and limited observational input.

14. SUBJECT TERMS: ADCP, SELFE, tidal currents, Columbia River	**15. NUMBER OF PAGES** 71
	16. PRICE CODE

17. SECURITY CLASSIFICATION OF REPORT	**18. SECURITY CLASSIFICATION OF THIS PAGE**	**19. SECURITY CLASSIFICATION OF ABSTRACT**	**20. LIMITATION OF ABSTRACT**
Unclassified	Unclassified	Unclassified	UU

NSN 7540-01-280-5500

Standard Form 298 (Rev. 2-89)
Prescribed by ANSI Std. 239-18

THIS PAGE INTENTIONALLY LEFT BLANK

Approved for public release; distribution is unlimited

CHARACTERIZATION OF THE VERTICAL STRUCTURE OF TIDAL CURRENTS IN THE MOUTH OF THE COLUMBIA RIVER AND EVALUATION OF THE SELFE MODEL

Joseph R. Oxendine
Lieutenant, United States Navy
B.S., University of North Carolina at Pembroke, 2003

Submitted in partial fulfillment of the
requirements for the degree of

MASTER OF SCIENCE IN METEOROLOGY AND PHYSICAL OCEANOGRAPHY

from the

NAVAL POSTGRADUATE SCHOOL
June 2014

Author: Joseph R. Oxendine

Approved by: Thomas H. C. Herbers
Thesis Advisor

Tim T. Janssen
Second Reader

Peter C. Chu
Chair, Department of Oceanography

THIS PAGE INTENTIONALLY LEFT BLANK

ABSTRACT

Lack of measurements has led to a poor understanding of tidal currents within the Mouth of the Columbia River (MCR). Shipboard ADCP measurements are a technically viable means to measure these currents and their vertical structures. Shipboard ADCP measurements from a three-week long cruise conducted by the R/V Point Sur are used in this study. Transects along the main shipping channel and across the bar were extracted using criteria of constant speed and heading. Vertical sections from each transect were compared with predictions from the SELFE model in order to evaluate the models' ability to predict these currents.

Observed flood currents within the river are bottom intensified with slight river outflow at the surface early in the flood cycle. Complete reversal of the flow throughout the column is experienced later as the flood fully develops. Ebb currents are much stronger and more homogenous throughout the water column due to the combination of river outflow and tidal current.

Inside the river mouth, the SELFE model agrees qualitatively well with observations, with only a few discrepancies. Outside the river mouth, the SELFE model does not resolve the observed vertical structure, possibly due to coarse grid resolution and limited observational input.

THIS PAGE INTENTIONALLY LEFT BLANK

TABLE OF CONTENTS

I. INTRODUCTION 1
A. MOTIVATION AND BACKGROUND 1
1. Tides 2
2. Tidal Currents in Coastal Regions 3
3. Non-Tidal Currents 5
4. Time Scales of Tidal and Non-Tidal Currents 5
5. Mouth of the Columbia River 6
a. The Columbia River 6
b. Bathymetric Features of MCR and Offshore Area 7
c. Tides and Tidal Currents within the MCR 8
B. NAVAL RELEVANCE 9
C. SCOPE 10

II. MODELING THE COLUMBIA RIVER 11
A. SELFE 11
B. SELFE PHYSICS 12
C. SELFE NUMERICS 13
D. IMPLEMENTATION WITHIN THE MCR 13

III. FIELD EXPERIMENT 17
A. DATA COLLECTION AND PREVIOUS RESEARCH 17
B. FIELD SITE 18
C. SHIPBOARD ACOUSTIC DOPPLER CURRENT PROFILER ARRANGEMENT 20
1. Measurement Principle 20
2. Shipboard ADCP Configuration 21
3. Post-Processing Ship Mounted Data 22

IV. DATA AND MODEL ANALYSIS 25
A. ADCP TRANSECTS 25
1. Selection Process 25
2. Selected Sections 26
B. SELFE MODEL DATA 27
C. FINAL SELECTION 28

V. FLOOD RESULTS 31
A. TRANSECT 1: PEAK FLOOD TO SLACK INSIDE MCR 32
B. TRANSECT 2: SLACK TO PEAK FLOOD INSIDE MCR 34
C. TRANSECT 5: FLOOD OUTSIDE OF MCR 37

VI. EBB RESULTS 39
A. TRANSECT 3: PEAK EBB TO SLACK INSIDE THE MCR 39
B. TRANSECT 4: SLACK TO PEAK EBB INSIDE THE MCR 42
C. TRANSECT 6: EBB OUTSIDE OF MCR 45

VII. CONCLUSION 47

A. SUMMARY 47
1. MCR Shipboard ADCP Measurements 47
2. Observed Vertical Structure 47
3. SELFE Model Evaluation 48
B. FUTURE RESEARCH 48
LIST OF REFERENCES 51
INITIAL DISTRIBUTION LIST 55

LIST OF FIGURES

Figure 1. Mouth of the Columbia River with the North and South Jetties labeled. (from *Wikipedia* cited 2014). 2
Figure 2. (A) Spring tides occur when the solar and lunar tractive forces are aligned with the Earth. (B) Neap tides occur when the solar and lunar tractive forces are at right angles to each other (from Bowditch 2002)..... 3
Figure 3. Flood and ebb currents within a harbor. Flood current flows upstream while ebb current flows downstream (from Gross 2005). 4
Figure 4. Time scales for different current driving mechanisms (from MetEd COMET Program). 6
Figure 5. The Columbia River estuary and bar with the North and South Jetties labeled (after CMOP cited 2014). 7
Figure 6. NOAA predicted tides for the period of 25May2013-01Jun2013 (from NOAA Tides cited 2014). 8
Figure 7. (a) Entire MCR SELFE model grid, (b) MCR estuary SELFE model grid, and (c) MCR tidal freshwater SELFE model grid (after Karna 2014). 12
Figure 8. Bathymetry for (a) Entire MCR SELFE model grid, (b) MCR estuary SELFE model grid, and (c) MCR tidal freshwater SELFE model grid (after Karna 2014). 15
Figure 9. The Mouth of the Columbia River with jetties, Columbia River bar, and Astoria-Megler Bridge labeled (after Google Earth, 2014). 18
Figure 10. USGS bathymetry of the bar and the MCR. The trench is well defined in the main navigation channel (after Stevens 2014). 19
Figure 11. a. Stationary Observer b. Moving Observer (from Simpson 2001)..... 20
Figure 12. The relationship of beam and Earth velocity components (from RD Instruments 1996). 22
Figure 13. Complete cruise track of the 2013 RIVET II Research Cruise..... 25
Figure 14. Image displaying the locations of all transects (white lines) (after Google Earth 2014)..... 27
Figure 15. Final six transects. (a) Shows all six transects. (b) Shows four transects within the MCR. (c) Shows two transects outside the MCR close to the bar (after Google Earth 2014). 29
Figure 16. Transects during flood inside the MCR (left panel) and outside the MCR (right panel)..... 31
Figure 17. Transect 1 vertical section plots for ADCP (top panel) and SELFE (bottom panel) data. Current speed is shown in color with positive values indicating up-river (flood) flow and negative values indicating down-river (ebb) flow. NOAA predictions of max flood current and times of max flood and slack water at Clatsop Spit station are indicated on the left. 33
Figure 18. Transect 1 current vectors for ADCP (top panels) and SELFE (bottom panels) data at 7.08 m (left panels) and 13.08 m (right panels) depth. 34
Figure 19. Transect 2 vertical section plots for ADCP (top panel) and SELFE (bottom panel) data. Current speed is shown in color with positive values

indicating up-river (flood) flow and negative values indicating down-river (ebb) flow. NOAA predictions of max flood current and times of max flood and slack water at Clatsop Spit station are indicated on the left. 36
Figure 20. Transect 2 current vectors for ADCP (top panels) and SELFE (bottom panels) data at 7.08 m (left panels) and 13.08 m (right panels) depth. 37
Figure 21. Transect 5 vertical section plots for ADCP observations (upper panels) and SELFE predictions (lower panels). Left panels: u component (+ eastward, - westward). Right panels: v component (+ northward, - southward)..... 38
Figure 22. Transects on the left represent ebb data inside the MCR while the transect on the right represents ebb data outside of the MCR. 39
Figure 23. Transect 3 vertical section plots for ADCP (top panel) and SELFE (bottom panel) data. Current speed is shown in color with positive values indicating up-river (flood) flow and negative values indicating down-river (ebb) flow. NOAA predictions of max ebb current and times of max ebb and slack water at Clatsop Spit station are indicated on the left. 41
Figure 24. Transect 2 current vectors for ADCP (top panels) and SELFE (bottom panels) data at 7.08 m (left panels) and 13.08 m (right panels) depth. 42
Figure 25. Transect 4 vertical section plots for ADCP (top panel) and SELFE (bottom panel) data. Current speed is shown in color with positive values indicating up-river (flood) flow and negative values indicating down-river (ebb) flow. NOAA predictions of max ebb current and times of max ebb and slack water at Clatsop Spit station are indicated on the left. 44
Figure 26. Transect 4 current vectors for ADCP (top panels) and SELFE (bottom panels) data at 7.08 m (left panels) and 13.08 m (right panels) depth. 45
Figure 27. Transect 6 vertical section plots for ADCP observations (upper panels) and SELFE predictions (lower panels). Left panels: u component (+ eastward, - westward). Right panels: v component (+ northward, - southward)..... 46

LIST OF ACRONYMS AND ABBREVIATIONS

ADCIRC	Advanced Circulation model
ADCP	Acoustic Doppler Current Profiler
CMOP	Center for Coastal Margin Observation and Prediction
CODAS	Common Ocean Data Access System
ELCIRC	Eulerian-Lagrangian Circulation model
GPS	Global Positioning Satellite
HYCOM	Hybrid Coastal Ocean Model
Hz	hertz
IMU	inertial motion unit
kHz	kilohertz
km	kilometer
m	meter
MCR	Mouth of the Columbia River
ms^{-1}	meters per second
m^3s^{-1}	cubic meters per second
NCEP	National Centers for Environmental Prediction
NCOM	Navy Coastal Ocean Model
NetCDF	Network Common Data Form
NRL	Naval Research Laboratory
NOAA	National Oceanographic and Atmospheric Administration
ONR	Office of Naval Research
RIVET II	River and Estuarine Transport II
SELFE	Semi-implicit Eulerian-Lagrangian Finite Element model
UHDAS	University of Hawaii Data Acquisition System
USGS	United States Geological Survey
UTC	Coordinated Universal Time
WRD	Wave Resolving Drifter

THIS PAGE INTENTIONALLY LEFT BLANK

ACKNOWLEDGMENTS

I would like to thank Professor Tom Herbers, first and foremost, for taking me on as a student and guiding me along. It was amazing to be able to participate in this research and collect my own data in the field, and I cannot express my gratitude for that opportunity enough. I wish him all the best in his future endeavors.

I would like to Dr. Tim Janssen for agreeing to be my second reader, and for his guidance and assistance during the field experiment.

I would like to thank Doug Pearman for his advice and friendship. His knowledge and excitement for the science was an inspiration to me. I would also like to thank Doug for his assistance and leadership during the field experiment as well.

I would like to thank Mike Cook for his assistance and guidance with many MATLAB issues. I would also like to say he has been one of my favorite teachers in my time at NPS.

I would like to thank Paul Turner and Toumas Karna at OHSU for their assistance in acquiring the SELFE model data, and interpretation of some of my results.

I cannot begin to say how much I appreciate Paul Jessen. His guidance and knowledge of MATLAB are second to none and he has been an absolute Godsend for this research. He is also one of the most outstanding field researchers I have ever worked with. I truly appreciate all he has helped me accomplish and wish him nothing but the best. Paul, you are a scholar and a gentleman.

Finally, I would like to thank my classmates. I could not think of a better group of individuals to have completed this program with. It has been my privilege and my honor to know each of them. I wish them fair winds, and following seas until we meet again.

THIS PAGE INTENTIONALLY LEFT BLANK

I. INTRODUCTION

A. MOTIVATION AND BACKGROUND

Coastal environments are vital areas of interest to all aspects of society. Important activities in the coastal zone include import and export of goods as well as commercial fishing, recreation on beaches and waterways, U.S. Coast Guard search and rescue and naval maritime operations, energy production and construction of coastal structures (piers, jetties, and bars). The study of these environments is important because a better understanding of their dynamics leads to safer navigation, more accurate chart production, safer design and building of coastal structures, and a better understanding of the evolution of coastal regions through currents and sediment transport.

One important aspect of coastal research is the study of tidal currents. The strength and orientation of these currents affect other important aspects of coastal environments such as sediment transport, bathymetry, and wave interactions at river mouths. The ability to accurately predict the behavior of currents throughout a tidal cycle is a key step toward safety of navigation, and the management of coastal regions.

This study focuses on the currents in the Mouth of the Columbia River (MCR) (Figure 1). The Columbia River is the largest river on the North American Pacific Coast. The river's strong outflow, coupled with its strong tidal currents, create an estuary at the mouth of the river with very dynamic oceanographic features, characterized by primarily broad shoals separating narrowing channels. Atmospheric processes are secondary in nature to the effects of river flow and tidal influence. Tidal currents in particular, are a dominant factor in determining the flow phenomena occurring within the estuary (Jay and Smith 1990).

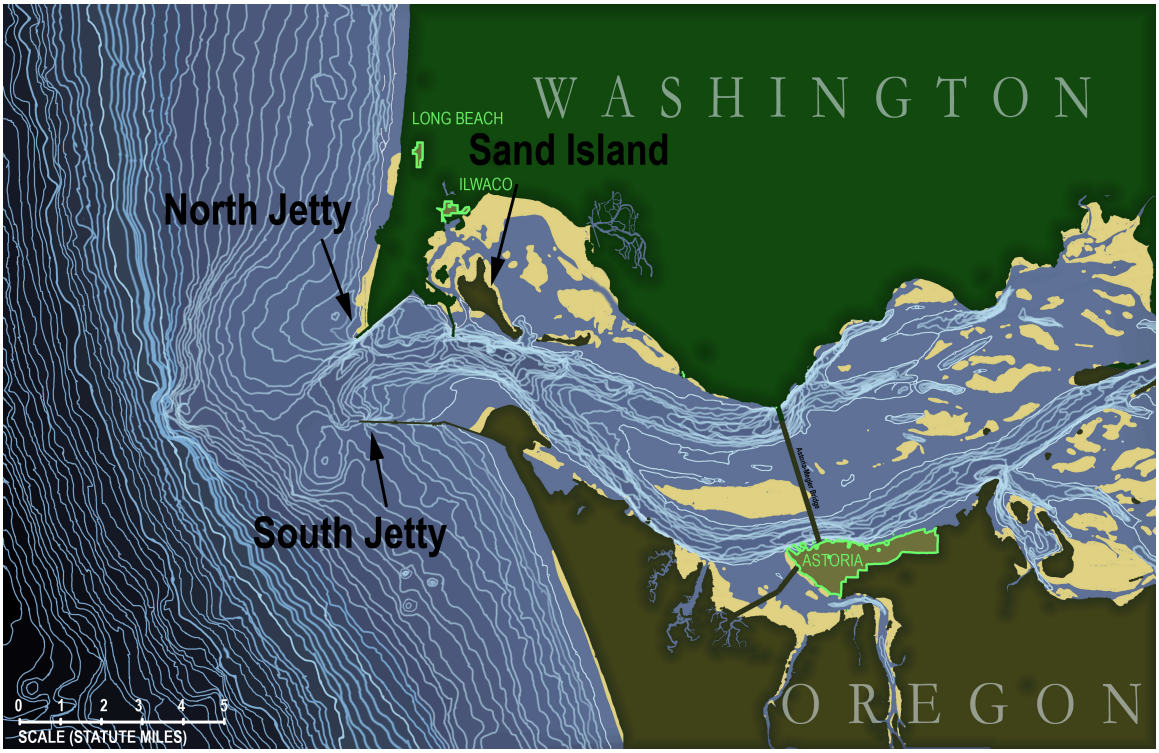

Figure 1. Mouth of the Columbia River with the North and South Jetties labeled. (from *Wikipedia* cited 2014).

1. Tides

Tides are the periodic rise and fall of the sea surface caused by gravitational attractive forces between the sun and moon and the rotating Earth. The moon's gravitational pull is the principle tide-generating force due to the sun's greater distance from Earth (Bowditch 2002).

Coastal regions all over the world experience one of three different types of tides; diurnal, semi-diurnal, and mixed tides (Gross 2005). Diurnal tides occur when a coastal region experiences only one high tide and one low tide per day (Gross 2005). Semidiurnal tides occur when a coastal region experiences two high tides and two low tides per day. Semi-diurnal tides are observed at the equator year round (Gross 2005). Mixed tides occur when a coastal region experiences two unequal high tides and low tides within a day.

The tidal range is affected by the alignment of the Earth-sun-moon system (Bowditch 2002). When the Earth, sun and moon are aligned the lunar and solar tractive forces combine to produce the greatest tidal ranges of the month called spring tides (Figure 2A). The sun and moon at right angles to the Earth result in the lowest tidal range of the month, called neap tides (Figure 2B.)

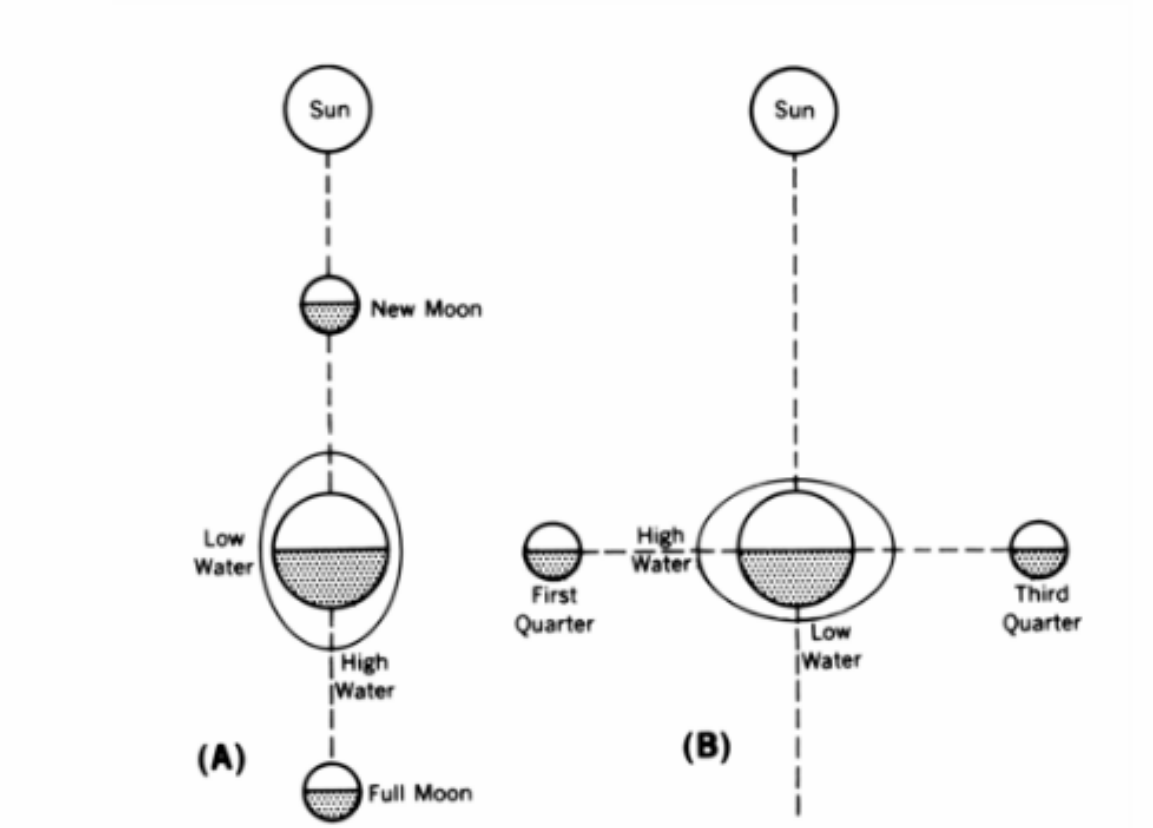

Figure 2. (A) Spring tides occur when the solar and lunar tractive forces are aligned with the Earth. (B) Neap tides occur when the solar and lunar tractive forces are at right angles to each other (from Bowditch 2002).

2. Tidal Currents in Coastal Regions

In coastal regions where flow is restricted by bathymetry such as channels or straits, tidal currents alternate between flood and ebb, filling and draining the bay or estuary (Figure 3). During slack water, the flow reversal between ebb and flood, the tide induced flows are very weak.

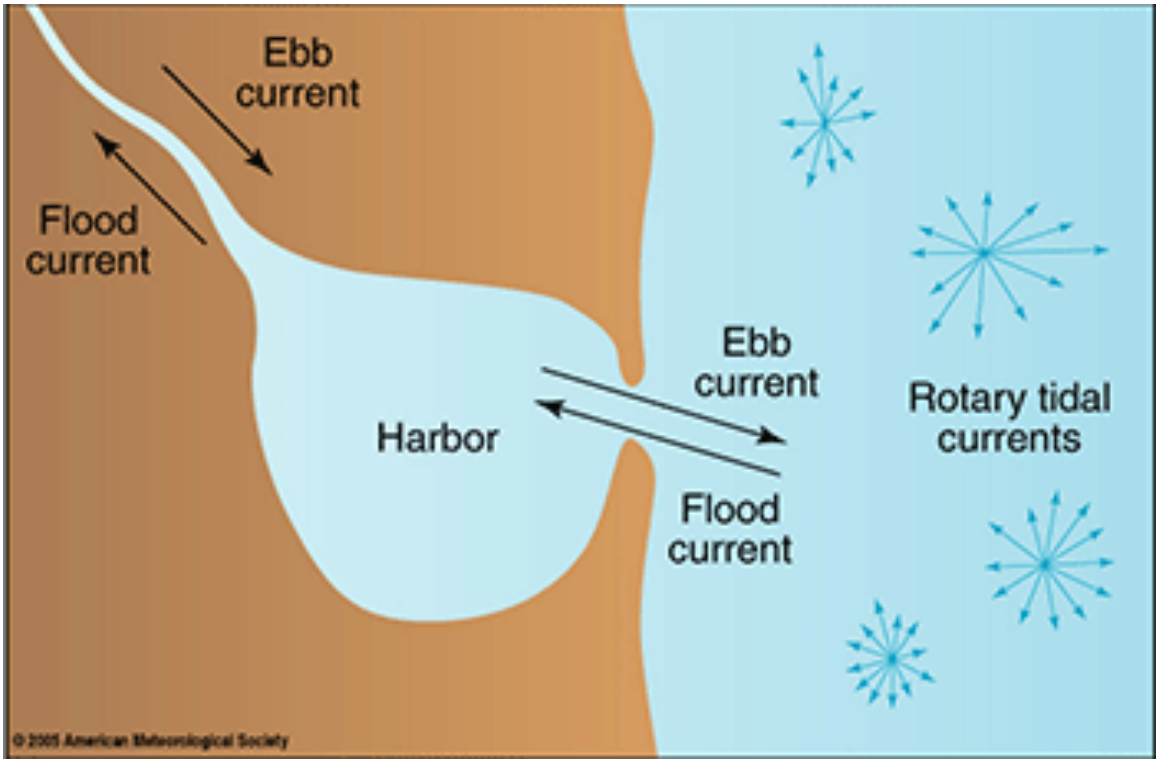

Figure 3. Flood and ebb currents within a harbor. Flood current flows upstream while ebb current flows downstream (from Gross 2005).

Like the tidal sea level variations, tidal currents are periodic in nature, with variations in amplitude over the tidal cycle. The strongest tidal currents occur during spring tides while the weakest tidal currents occur during neap tides (Gross 2005). This periodicity exhibited by tidal currents distinguishes them from other non-tidal currents. Other variations in tides and tidal currents occur as a result of the moon's continuous changes in phase (29.5 days), distance from the Earth (27.5 days), and declination to the Earth (27.3 days) (Disney and Overshiner 1925). Changes in the moon's phase and distance from Earth cause changes in tidal current strength that are approximately proportional to changes in tidal range. Changes in the moon's declination, however, lead to changes in tidal current strength that are approximately half of the changes in tidal range (Disney and Overshiner, 1925).

3. Non-Tidal Currents

Non-tidal constituents in the form of river outflow and wind-driven currents usually accompany tidal currents in coastal regions. Wind drives surface currents that decrease with depth due to seabed friction. Temperature differences between two separate bodies of water, as well as density differences between freshwater and salt water, cause horizontal stratification within the water column that leads to density driven currents (Koch and Sun 1999).

4. Time Scales of Tidal and Non-Tidal Currents

Tidal and non-tidal current time scales are shown in Figure 2. Density driven currents operate over many different time scales depending on the forcing mechanisms. Ebb tides can transport fresh water into estuaries or out onto continental shelves over short time periods. Flash floods resulting from rainfall can last for days. Seasonal processes such as runoff and evaporation can last as long as the season in which they are happening, weeks or more. Tidal and wind driven currents in coastal areas often have similar time scales because of the diurnal cycle of the sea breeze.

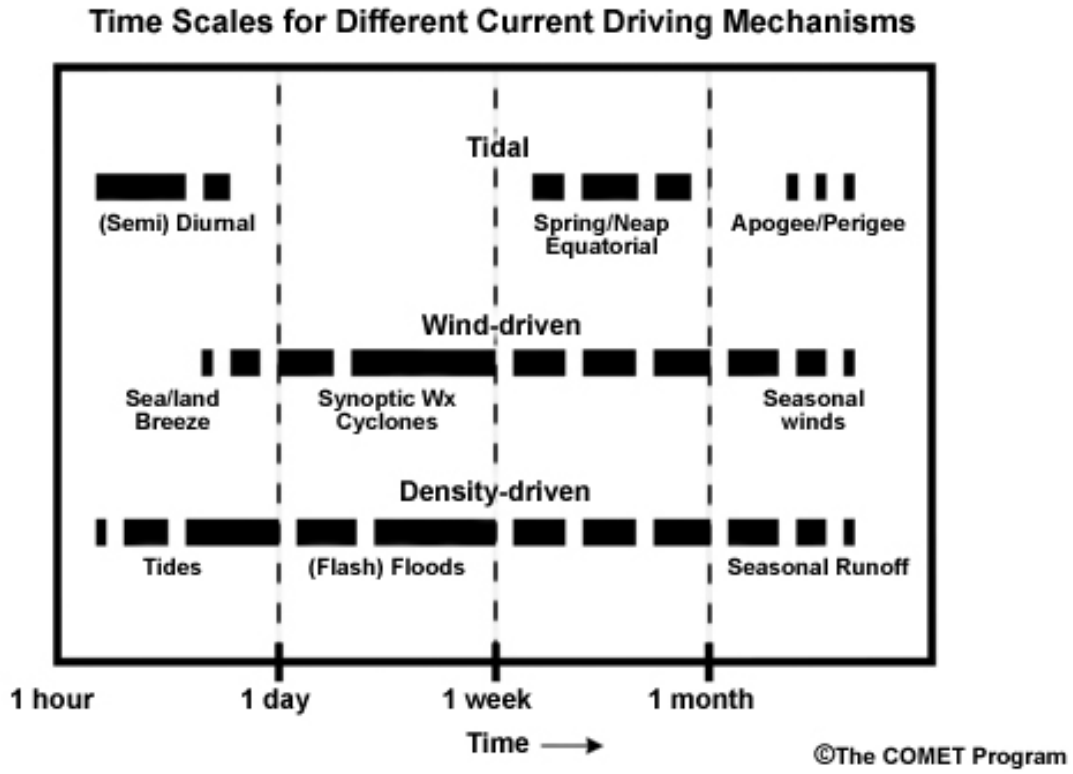

Figure 4. Time scales for different current driving mechanisms (from MetEd COMET Program).

5. Mouth of the Columbia River

a. The Columbia River

The Columbia River drainage basin covers an area approximately 660,480 km^2 in seven U.S. states and two Canadian provinces (Simenstad et al. 2002). With an average discharge of approximately 7,300 m^3sec^{-1}, the Columbia River is the largest river on the U.S. Pacific coast and the fourth largest river in the U.S., by volume (Jay et al. 1984). The Columbia River originates in the Rocky Mountains of British Columbia and flows in a mean southern direction to empty out into the Pacific Ocean along the Washington-Oregon border in the northwest U.S. The river's large flow rate, combined with a steep gradient from its mountainous, decent gives the Columbia River tremendous potential for generating hydroelectric power. The river has been dammed hundreds of times in the last century for hydroelectric power generation, irrigation, and flood control (Elias et al. 2012).

b. Bathymetric Features of MCR and Offshore Area

The Columbia River bar extends offshore from the mouth of the river approximately 8 km. It is a relatively flat, and shallow (~20 m) region that is radially symmetric about the tip of the North Jetty (Kilcher and Nash 2010). The estuary is constricted at the mouth of the river by two jetties: the North Jetty located at the tip of Peacock Spit and the South Jetty located at the tip of Clatsop Spit. The river narrows from 10 km within the estuary to 3.5 km at the mouth of the river before flowing into the Pacific Ocean (Kilcher and Nash 2010). The estuary is also rather shallow except for the two shipping channels that cut through the bar and run through the estuary. The North Channel splits from the main channel and touches on the southern coast of Washington within the estuary. The main Navigation Channel hugs the southern edge of the estuary and continues upriver southeast. Both shipping channels average 20 m depth and are the deepest points within the estuary (Figure 5).

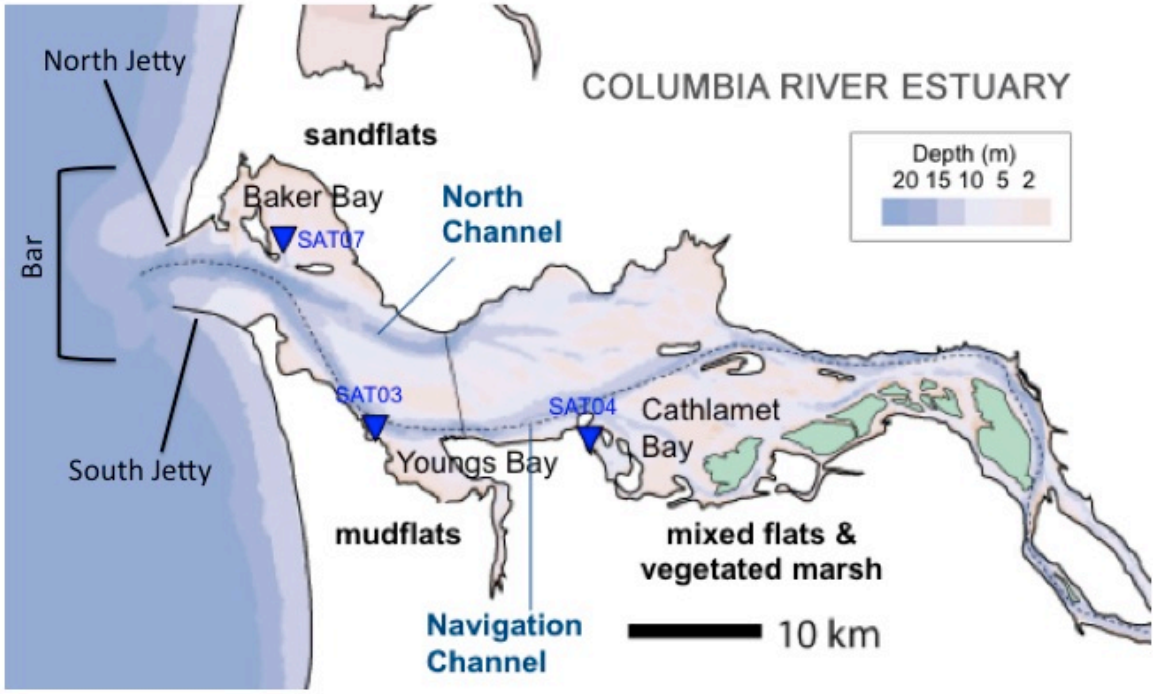

Figure 5. The Columbia River estuary and bar with the North and South Jetties labeled (after CMOP cited 2014).

c. Tides and Tidal Currents within the MCR

Tidal forcing dominates the dynamics within the estuary, but river flow takes on an increasingly important role upriver from the entrance. The Columbia River is affected by tides, as far as 243 km upriver from the mouth (Templeton and Jay 2013). Tides within the MCR are mixed, consisting of two high waters and two low waters over a 24.8 hour period, with a mean diurnal range of approximately 1.8 m (Jay et al. 2011). At the mouth of the river the mean and diurnal tidal ranges are 2 m and 2.6 m, respectively (Lutz et al. 1975). Figure 6 depicts NOAA predicted tides at the Hammond, OR station for the period of 25 May 2013 to 01 Jun 2013. This is a typical mixed, semi-diurnal tidal range experienced in this coastal region.

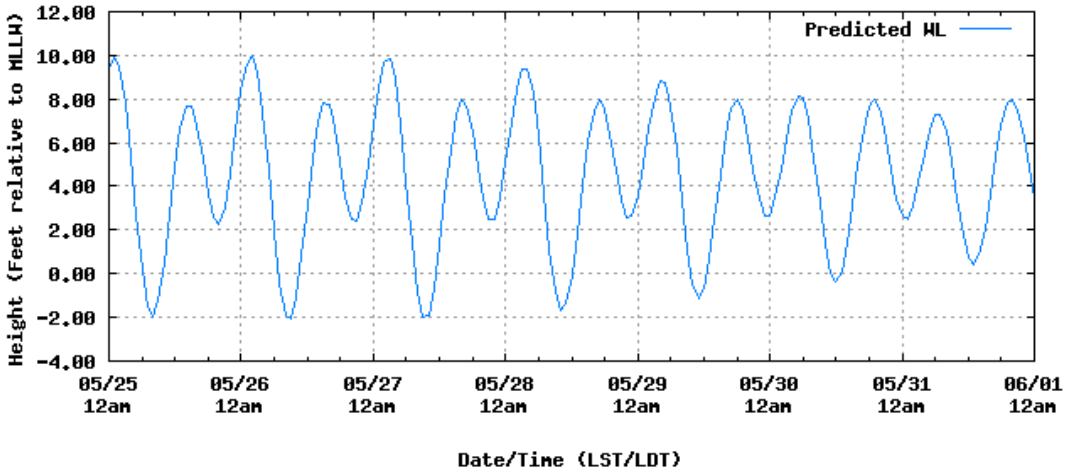

Figure 6. NOAA predicted tides for the period of 25May2013-01Jun2013 (from NOAA Tides cited 2014).

Tidal currents are stronger within the North Channel because most of the tidal prism of the lower estuary is filled from the North Channel (Jay and Smith 1990). Much of the tidal transport is applied to fill the tidal prism over the estuary, and therefore, tidal current velocities decrease strongly upriver (Jay and Smith 1990). During the ebb cycle, surface currents can routinely reach up to and exceed 2-3 ms^{-1} causing a significant increase in the height and steepness of opposing surface waves in a matter of less than 2-3 hours

(Gonzales 2000). In regions where the water column is well mixed, bottom friction slows the currents greatly, leading to velocities decreasing with depth from the surface.

Strength of the river flow also tends to have an effect on tidal currents. When non-tidal constituents such as river flow and wind forcing are not considered, ebb and flood periods and magnitudes are approximately equal. The strength of the Columbia River flow, however, acts to increase the strength of the ebb current while decreasing the strength of the flood current. River flow also impacts the length and time period, of the tidal cycles, causing ebb duration to increase and flood duration to decrease (Bowditch 2002).

B. NAVAL RELEVANCE

The Columbia River bar is one of the major landmarks of the infamous "Graveyard of the Pacific". This region is characterized by intense wave-current interactions, and has been recognized as one of the most dynamic and dangerous coastal regions in the entire world. With an annual passage of approximately 2,000 vessels, safety of navigation through the channel has become paramount (Simenstad et al. 2002).

Cape Disappointment, located just north of Peacock Spit, is home to Coast Guard Station Cape Disappointment. Gonzales (1984) notes that statistics from this station showed that an average of 850 search-and-rescue missions were conducted each year. The construction of the North and South jetties at the entrance of the river greatly improved navigation but shifted the morphology of the inlet. Because of this, dredging is required to maintain the channel depth at its required 17 m. The jetties require frequent maintenance due to severe wave and tide interactions (Elias et al. 2012).

Safety of navigation is important through this region because of the dynamic environmental conditions, but also because of the regional economic situation. The ports of Portland and Vancouver are accessed via the Columbia River. Research from Jay et al. (2011) reveals that ongoing changes in water levels and tidal ranges affect ships draft within the channel as well as shallow-water habitat. Decreasing water levels coupled with increasing ship drafts lead to an increase in difficulty, and risk navigating the Columbia River.

C. SCOPE

The goals of this research are twofold: characterize the vertical structure of tidal currents within the MCR over various tidal cycles, and validate the SELFE model's ability to predict these currents.

Characterizing the vertical structure of the tidal currents is important because of the strong stratification typically found in river mouths. Saline water from the ocean is denser than fresh water from upriver, so this difference in density causes strong shear throughout the column as these two water masses meet (Elias et al. 2012). The ADCP measurements collected onboard the R/V Point Sur in the ONR RIVET II Experiment provides an opportunity to investigate the vertical structure of tidal currents in the MCR.

Despite the significant economic and social importance of the MCR, relatively few detailed measurements of the tidal flows have been reported. As a result, little is known about its vertical tidal structure.

Evaluating operational models of the MCR circulation such as the SELFE model, tested in this research, will provide mariners with a more accurate depiction of the tidal current variability within the river mouth. Understanding these currents and their structure, and helping to validate a model that can eventually be used as a regular navigation tool is a step in the direction to safer navigation within the estuary.

II. MODELING THE COLUMBIA RIVER

A. SELFE

There are a few models currently in use to predict hydrodynamic conditions within the Columbia River estuary. The Semi-implicit Eulerian-Lagrangian Finite Element model (SELFE) is an operational modeling system that is a refinement of the well-established Eulerian-Lagrangian Circulation model (ELCIRC) (Burla et al. 2010a). This semi-implicit, unstructured grid model solves the 3D barotropic shallow-water equations and can be used to predict 3D velocities, water levels, temperature, and salinity at each point in space and time over the entire computational domain (Burla et al. 2010b). SELFE utilizes a finite-element framework with a terrain-following coordinate system approaching the bottom boundary layer (Burla et al. 2010b).

The SELFE model came about by efforts to improve older unstructured grid models such as ELCIRC (Zhang and Baptista 2008). SELFE retains many important base features from previous models to include computational efficiency from semi-implicit Eulerian-Lagrangian finite volume modeling, but allows for superior flexibility in representing bathymetry by relaxing restrictions on grids, and using higher-order shape functions to calculate elevations (Zhang and Baptista 2008). SELFE can utilize either *S* coordinates or hybrid *SZ* coordinates to represent a vertical grid that resembles unstructured grids, which allow for superior representation of bathymetry and vertical structure of the water column (Zhang and Baptista 2008). SELFE solves for 3D velocity, 3D temperature and salinity, and free-surface elevation (Zhang and Baptista 2008). Figure 7 shows the MCR SELFE model domain grid.

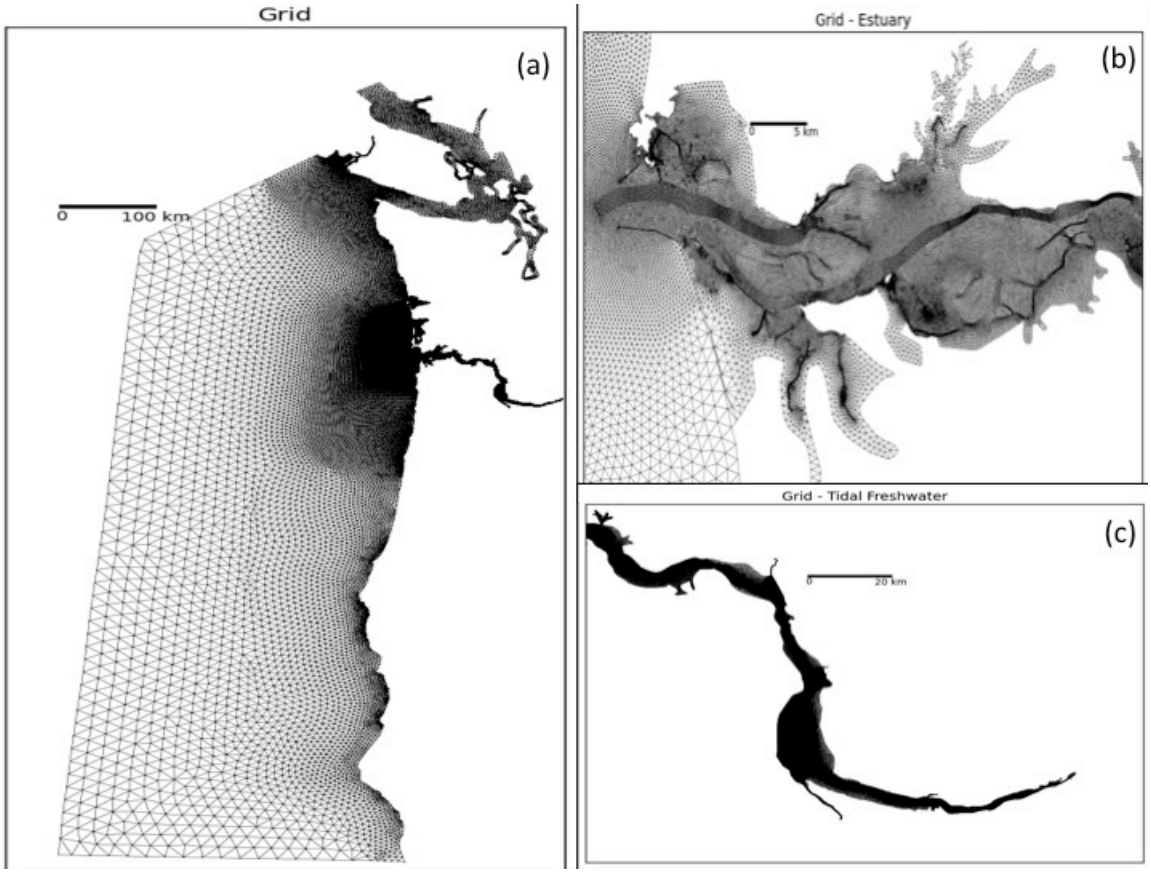

Figure 7. (a) Entire MCR SELFE model grid, (b) MCR estuary SELFE model grid, and (c) MCR tidal freshwater SELFE model grid (after Karna 2014).

B. SELFE PHYSICS

SELFE solves for the 3D shallow-water equations by using a combination of the hydrostatic and Boussinesq approximations, as well as transport equations for salt and heat (Zhang and Baptista 2008). The Generic Length Scale turbulence closure of Umlauf and Burchard (2003) is used to calculate turbulence within SELFE.

Most ocean models perform poorly at resolving the bottom boundary layer when using the no-slip condition, ($u=w=0$). SELFE, however, uses a balance between the internal Reynolds stress and the bottom frictional stress to resolve the bottom boundary layer (Zhang and Baptista 2008). Different boundary layers (i.e., laminar vs. turbulent) may require different forms of bottom stress (Zhang and Baptista 2008). SELFE is

flexible enough to be applied to various boundary layer types and bottom stresses (Zhang and Baptista 2008).

C. SELFE NUMERICS

SELFE has several advantages over its predecessors that enhance numerical efficiency and accuracy. First, SELFE solves the shallow water equations system described above using a finite-element and finite-volume scheme (Zhang and Baptista 2008). This eliminates the requirement for splitting the internal and external modes, thus eliminating errors that are related with mode splitting (Shchepetkin and McWilliams 2005). Second, advection terms within the momentum equations are treated using an Eulerian-Lagrangian method which reduces numerical stability constraints (Zhang and Baptista 2008). Finally, SELFE uses a semi-implicit scheme to all equations, while solving the continuity and momentum equations simultaneously, eliminating stability restrictions associated with previous models (Zhang and Baptista 2008).

D. IMPLEMENTATION WITHIN THE MCR

Within the MCR, SELFE is used to produce data via the application of the model to a variety of inputs. River discharges at Bonneville Dam are from the U.S. Army Corps of Engineers, while other river inputs are from U.S. Geological Survey (USGS) instrumentation throughout the river and estuary (Turner 2014).

Atmospheric conditions, air temperature, solar flux, and winds are taken from the National Centers for Environmental Prediction (NCEP) North American Regional Reanalysis (NARR). This database contains data sets from numerical weather predictions to include model outputs, weather model outputs and inputs, as well as climate model data sets (Turner 2014).

Ocean boundary conditions for salinity, temperature, and sea surface height come from two different models depending on the dates of the data (Turner 2014). Data from years prior to 2013 are acquired from the Naval Research Laboratories Navy Coastal Ocean Model (NCOM). This model has since been retired and all subsequent data come from Hybrid Coordinate Ocean Model (HYCOM) (Turner 2014).

Tides are provided to SELFE via the Advanced Circulation model (ADCIRC) (Turner 2014). ADCIRC is a finite element hydrodynamic model based on unstructured grids similar to SELFE (Meyers and Baptista 2001). ADCIRC applies variable resolution, which allows the model to transition between a coarser representation in deeper ocean environments and a finer representation in nearshore environments (Meyers and Baptista 2001).

Bathymetry within SELFE is a composite of multiple sources. Bathymetry is loaded to the model grid sequentially from the following progressively higher resolution data sets:

- NGDC ETOPO2v2
- NGDC 3arc second Coastal Relief Model
- NGDC 1/3 arc second raster for LaPush, Taholah, and Astoria
- DOGAMI combined bathymetry and LiDAR dataset for the Columbia River Estuary up to Bonneville and Willamette Falls
- USACE 2012 bank to bank survey (from Jetty A to Tongue Point)
- USACE yearly cross channel surveys for the area around the navigation channel
- USACE monthly along channel surveys for the navigation channel.

Figure 8 shows the MCR SELFE bathymetry grid.

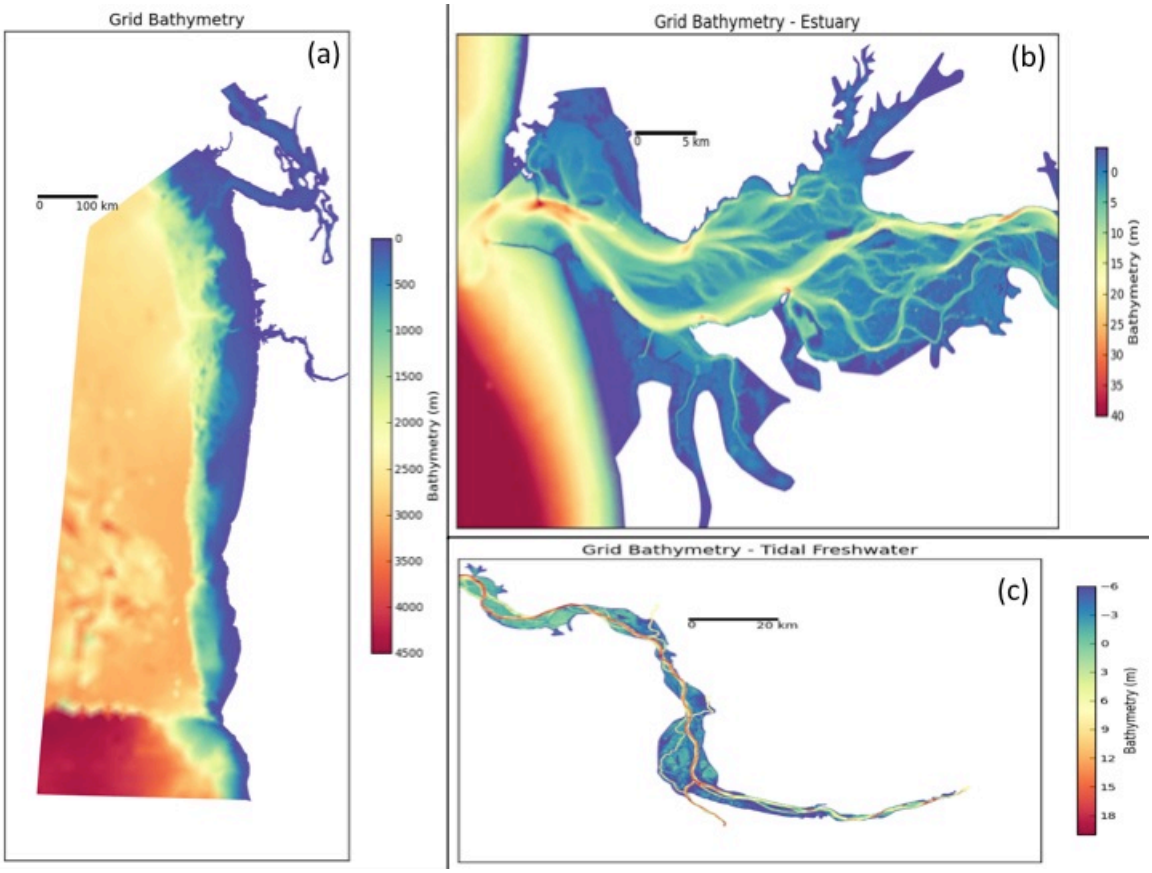

Figure 8. Bathymetry for (a) Entire MCR SELFE model grid, (b) MCR estuary SELFE model grid, and (c) MCR tidal freshwater SELFE model grid (after Karna 2014).

THIS PAGE INTENTIONALLY LEFT BLANK

III. FIELD EXPERIMENT

A. DATA COLLECTION AND PREVIOUS RESEARCH

Data for this research were collected during the Office of Naval Research (ONR) sponsored RIVET II Experiment in the MCR. The focus of this project, involving scientists from many institutions, is the hydrodynamic and morphodynamic processes resulting from waves, tidal currents and river outflow in this complex estuary. The NPS team in collaboration with Thesis Research (Dr. Tim Janssen) was responsible for collecting in-situ wave and current measurements.

The data used in this research were collected during a research cruise within the MCR from 25 May 2013 to 14 Jun 2013 aboard the scientific research vessel R/V Point Sur. Pearman (2014) researched wave evolution within river mouths and tidal inlets via data collected by a fleet of Wave Resolving Drifters (WRDs) that were deployed and recovered several times over the course of the cruise. Three slightly different variants of the drifters were used to measure currents and waves via various onboard arrangements of equipment to include GPS loggers, accelerometers, and Inertial Motion Units (IMU). The drifters measured horizontal orbital velocities in the swell band, as well as vertical accelerations of higher-frequency wind waves (Pearman 2014).

Portell (2013) validated the use of IMUs as an accurate, and low-cost alternative for use in recording surface waves. Data collected from the WRDs deployed during this experiment were also used to help validate the results Portell (2013) concluded in his experiments. Portell (2013) constructed a wave simulation device to test IMUs at multiple wave frequencies and unit configurations within a laboratory setting. These results were compared to observations obtained from IMUs deployed during the experiment to estimate error analysis and accuracy (Portell 2013).

Finally, ADCP data were collected from both a shipboard mounted ADCP unit, as well as a bottom-moored ADCP unit. Data from these units were collected at a rate of one profile every two minutes. The shipboard ADCP data will be used here to characterize the vertical structure of the tidal currents within the MCR. These data will

also be compared to the SELFE model representations of the MCR in order to validate the accuracy of the model within this region.

B. FIELD SITE

All of the data used in this research were collected in the main Navigation Channel located in the southern portion of the Columbia River estuary, and just outside of the estuary off the bar (Figure 9). Transects inside the mouth of the river were collected in the region of the estuary between the entrance (North and South Jetties) to the estuary and the Astoria-Megler Bridge.

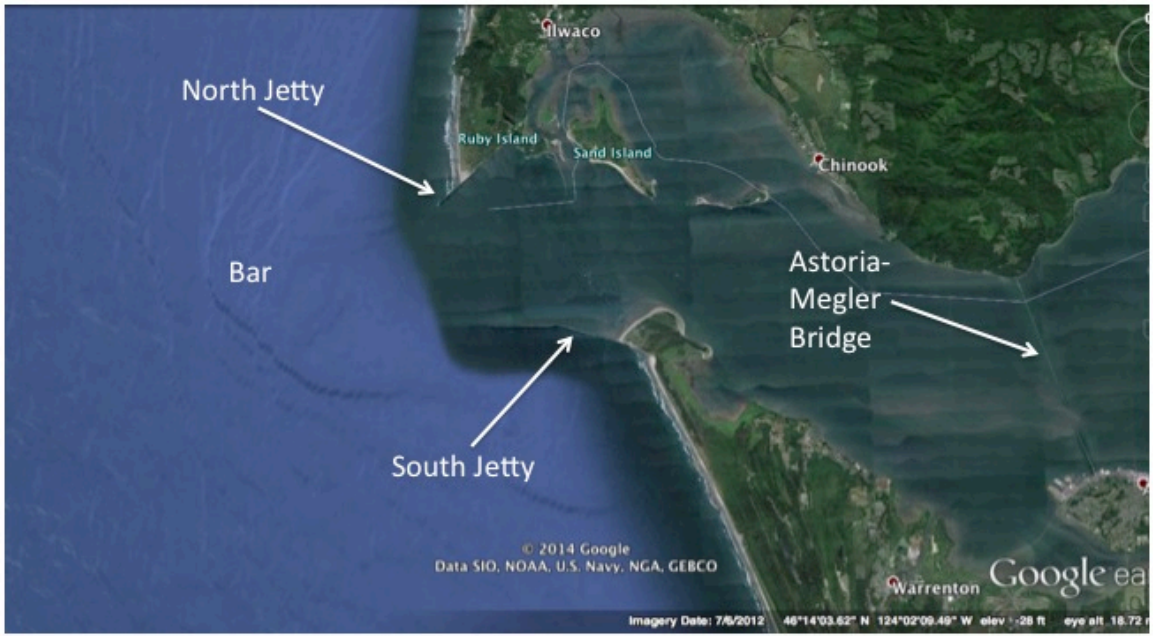

Figure 9. The Mouth of the Columbia River with jetties, Columbia River bar, and Astoria-Megler Bridge labeled (after Google Earth, 2014).

This region was chosen because this is the portion of the estuary where the rivers strong discharge begins to enter into a more narrow and constricted region of the estuary. The jetties funnel the flow through in a jet-like current that, during ebb currents, can routinely reach, and exceed, 2 m/s (Gonzales 1984). The bar (Figure 10) that has formed outside of the MCR as a result of these intense wave-current interactions and high volume sediment transport, has been one of the main causes of approximately 2,000 ships

being lost at sea in this region since 1792 (Simenstad et al. 2002). The bar extends offshore from the mouth of the river approximately 8 km. Its flat, shallow nature in contrast to the surrounding waters makes navigating this bar a treacherous ordeal. The Navigation Channel has been dredged through the southern point of the bar leading into the MCR. The channel depth averages 17-20m through the bar and continues on into the MCR to bifurcate into the North and South Channels. The South Channel is the main navigation channel. At approximately -123.95° longitude there is a trench within the South Channel that is approximately 20-25 m deep (almost 10 m deeper than the surrounding water).

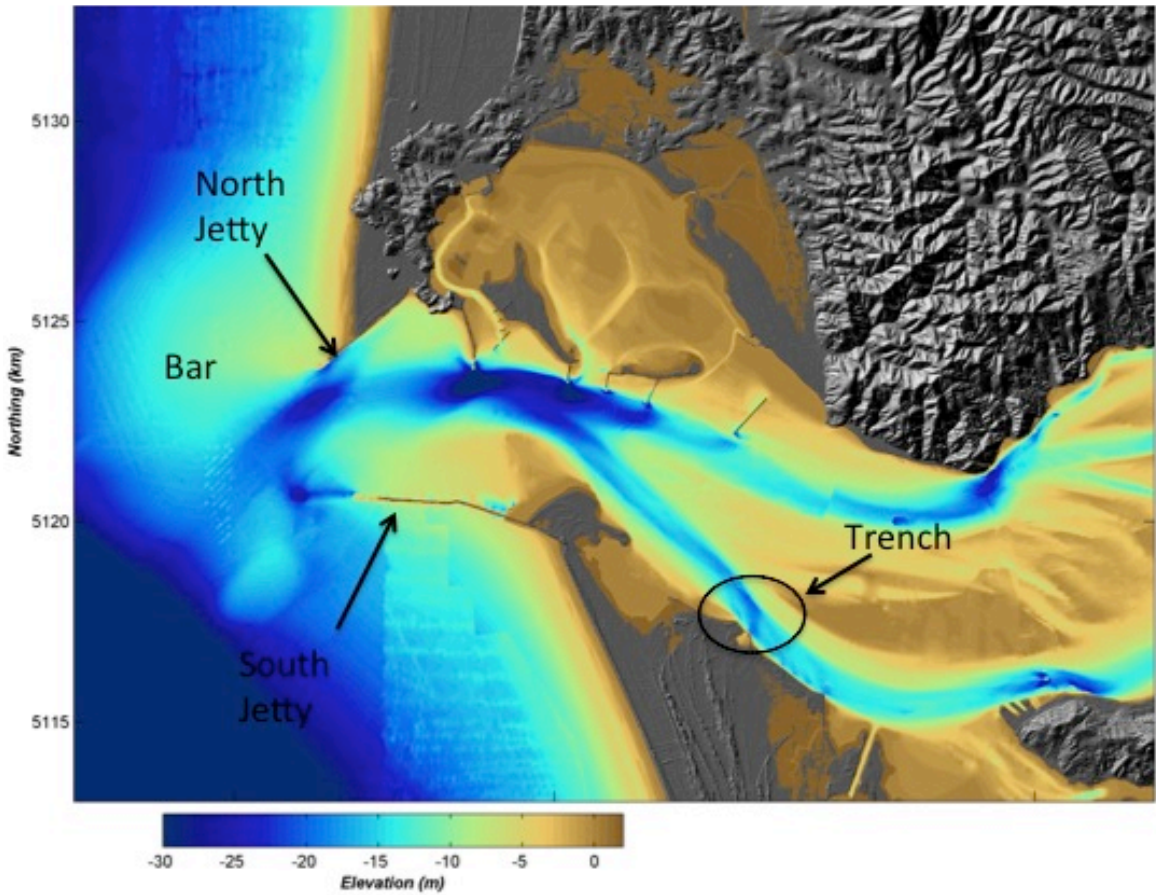

Figure 10. USGS bathymetry of the bar and the MCR. The trench is well defined in the main navigation channel (after Stevens 2014).

C. SHIPBOARD ACOUSTIC DOPPLER CURRENT PROFILER ARRANGEMENT

1. Measurement Principle

The Acoustic Doppler Current Profiler (ADCP) is the most commonly used instrument by oceanographers to measure currents within a water column. The instrument is popular for a multitude of reasons to include a wide variety of operating frequencies and depths, a well-tested and documented history of accuracy and performance, and the ease with which the instrument can be deployed in various configurations (i.e., hull-mounted, over-the-side, and bottom-moored) (RD Instruments 1996).

ADCPs work by using the Doppler effect to measure the relative radial velocity between different objects (Wewetzer et al. 1999). The Doppler effect is the observed change in frequency of a wave to an observer moving relative to its source. The Doppler principle can be described using a water wave in the following analogy. A stationary observer (Figure 11a.) is sitting on the surface of the water and notices that waves are passing his position a rate of one wave per second. If the observer begins to move in the direction of the source of the waves at a rate of four waves per second (Figure 11b), he will perceive a passage of five waves per second, even though the frequency of wave emission has not changed (Simpson 2001).

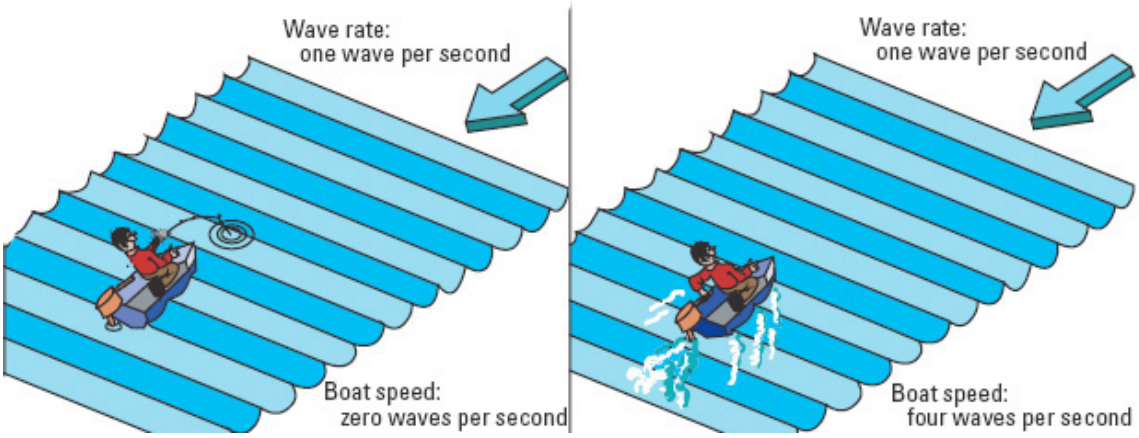

Figure 11. a. Stationary Observer b. Moving Observer
(from Simpson 2001)

ADCPs utilize the Doppler effect by transmitting sound at a fixed frequency through the water column and listening for the echoes returned from various 'scatterers' or suspended particles within the column (RD Instruments 1996). The particles are assumed to be of such size and strength that they move with the water so that their velocities are representative for the fluid velocity.

2. Shipboard ADCP Configuration

The vertical structure of ocean currents is often measured with an ADCP mounted to the hull of a ship. In this configuration the sensor is used to measure the movement of particles suspended within the water column relative to the ADCPs position. The navigation system is used to remove ship's motion from the ADCP data during post-processing to estimate the ocean currents in a fixed reference frame.

The R/V Point Sur is equipped with a Teledyne RD Instruments' Workhorse Mariner ADCP that operates at 300 kHz with a typical ping rate of 2 Hz (Teledyne 2014). Depth cell size for this data was set at 2 m, which yields a range of 78-102 m with a single ping standard deviation of 6.1 cm/s (Teledyne 2014). Further information on the 300 kHz unit's performance, accuracy, and resolution can be found at the following link:

http://marineops.mlml.calstate.edu/sites/default/files/wh_mariner_ds_lr.pdf

The WH 300 ADCP unit is mounted to the bottom of the R/V Point Sur hull at mid-ship. The unit is mounted such, that it can be accessed both internally (transducer electronics access) and externally (biofouling removal). The unit is recessed so as to not protrude past the hull. This protects the ADCP from debris damage, and minimizes the effect of air bubble attenuation across the path of the ADCP beams. Attenuation (weakening) of the signal by air bubbles reduces the profiling range and thus performance (RD Instruments 2002).

The WH 300 ADCP unit utilizes four sound beams to measure current velocity in three dimensions. Data is divided in evenly spaced segments throughout the water column called bins. This aspect of data collection makes the ADCP very similar to a moored line of standard current meters. The ADCP uses its four transducers to measure

horizontal velocity as well as vertical velocity of the currents (Figure 12). When the instrument beams are aligned to Earth coordinates, one pair of beams measures the north-south component of velocity while the other pair of beams measures the east-west component of velocity. While each pair of beams measures a different component of horizontal velocity, both pairs of beams are simultaneously measuring vertical velocity as well (RD Instruments 1996). This is where ADCPs differ greatly from standard current meters. Taking the sum of opposing beams cancels the horizontal velocities leaving only vertical velocities. Since these vertical velocities are assumed to be negligible they can thus be used as an error check (Wewetzer et al. 1999).

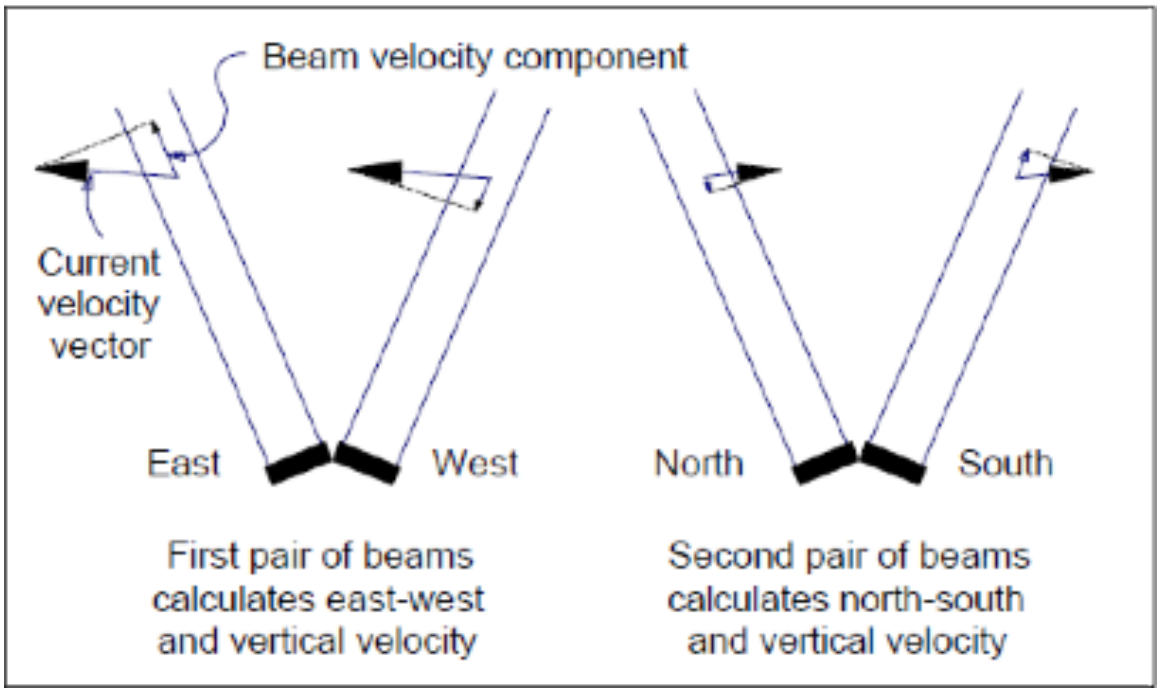

Figure 12. The relationship of beam and Earth velocity components (from RD Instruments 1996).

3. Post-Processing Ship Mounted Data

Data collected from a ship-mounted ADCP requires the correction of two types of motion: rotation (pitch, roll, and heading), and translation (ship velocity). Rotation correction is needed because the ship's pitch and roll affect the orientation of the beams and thus the velocity components that are being measured. These distortions are

compounded with an increase in severity of surface conditions (RD Instruments 1996). Translation correction is also essential because the ship's velocity, if moving, is usually greater than the actual current velocity (RD Instruments 1996).

The University of Hawaii has developed a suite of post-processing codes called UHDAS (University of Hawaii Data Acquisition System) that acquire data from the ADCP and ancillary sensors such as GPS, gyrocompass, and inertial attitude sensors and use CODAS (Common Ocean Data Access System) to build a dataset via user specified configurations. CODAS, through a series of editing steps, initially uses a reliable heading source such as a gyro to correct for heading errors, find UTC times of all data points, and edit out bad single-ping velocities. Finally, the reference layer is found and smoothed, bottom-track/water-track analysis is used to determine preliminary angle and amplitude corrections, bad data caused by bottom interference, or bubbles, are edited out, notes can be produced for later use, and the data files are extracted into a NetCDF format for use in MATLAB. Further information on the UHDAS Suite and CODAS post-processing method can be found at the following website:

http://currents.soest.hawaii.edu/docs/doc/index.html#

THIS PAGE INTENTIONALLY LEFT BLANK

IV. DATA AND MODEL ANALYSIS

A. ADCP TRANSECTS

1. Selection Process

To investigate the vertical structure of tidal currents, the shipboard ADCP data was broken up into transects where the ship was traversing the area of interest at a nearly constant heading. The complete ship track shown in Figure 13 contains numerous transects in the shipping channels and across the bar when the ship was conducting drifter deployments.

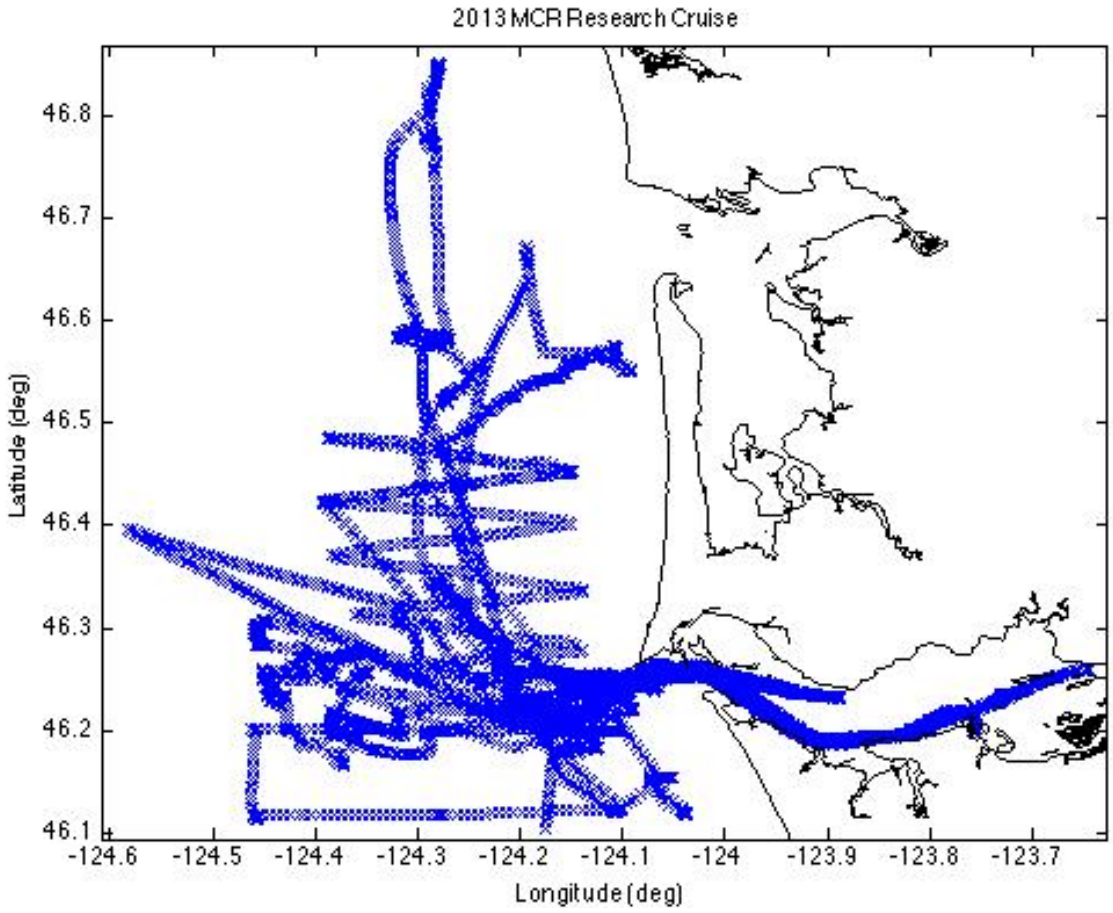

Figure 13. Complete cruise track of the 2013 RIVET II Research Cruise.

The first step involved breaking the entire data set down into transects. This was achieved by an automated termination of transects when the ship performed a change in heading greater than a user-specified maximum. The ADCP logged profiles at two-minute intervals, and heading changes were measured between successive profiles. The transects were terminated when the heading changed more than 30 degrees. To consider only transects with sufficient duration in the analysis, transects shorter than 40 minutes were discarded.

Next, transects were manually checked for their geographical location. As seen in Figure 13, most of the data collected was collected outside of the MCR. Only transects that were located outside of the river in close proximity to the bar, and inside the MCR between the Astoria-Megler Bridge and the jetties, were kept. Any transects located outside of the MCR away from the bar, and too far upriver were discarded.

Finally, all transects were manually checked for speed. Large decreases in ship's speed could possibly indicate the ship holding station. As with heading, speed was calculated using successive points within the data. Transects that exhibited changes in speed greater than 3 m/s or near zero speed were discarded.

2. Selected Sections

Once the selection process was complete, vertical section plots were generated that display the current magnitude and direction with longitude vs. depth. Of the 16 transects (Figure 14) that were kept, 11 of them were located in the main shipping channel between the mouth of the river and the Astoria-Megler Bridge. The remaining five transects are offshore over the bar area and its approaches

Predicted tidal currents were retrieved from NOAA archives for the Clatsop Spit station. This data contains the predicted magnitude and times for peak ebb and flood currents as well as slack water. The start and ending times for each transect were used in conjunction with the predicted tidal current data to identify what phase of the tidal cycle each transect was occurring in.

Figure 14. Image displaying the locations of all transects (white lines) (after Google Earth 2014).

Transects were initially divided according to their geographical location: inside the MCR and outside the MCR. Next, all transects were further divided into transects occurring during flood, and transects occurring during ebb. Finally, transects were further divided according to their proximity to slack water:

- Transects that have experienced slack water and are approaching peak flood.
- Transects that have experienced peak flood and are approaching slack water.
- Transects that have experienced slack water and are approaching peak ebb.
- Transects that have experienced peak ebb and are approaching slack water.

Transects were divided in this manner because one of the goals of this research was to characterize the vertical structure of the tidal currents during different tidal stages.

B. SELFE MODEL DATA

To help limit the size of the model data files, SELFE model data was extracted based on the times and locations of the observational transects. Once all the model data

were extracted for each ADCP transect, a model transect was constructed by choosing the nearest model grid point in space and time for each ADCP profile.

C. FINAL SELECTION

Comparisons between the observational data and the model were made for all 16 transects. A subset of these transects that characterized the vertical structure at each tidal stage are presented in the next two chapters. Transects were purposely chosen during early and late flood and ebb periods to illustrate the difference in flow structure in different parts of the tidal cycle. These final six transects (four inside the river and 2 outside the river) are shown in Figure 15.

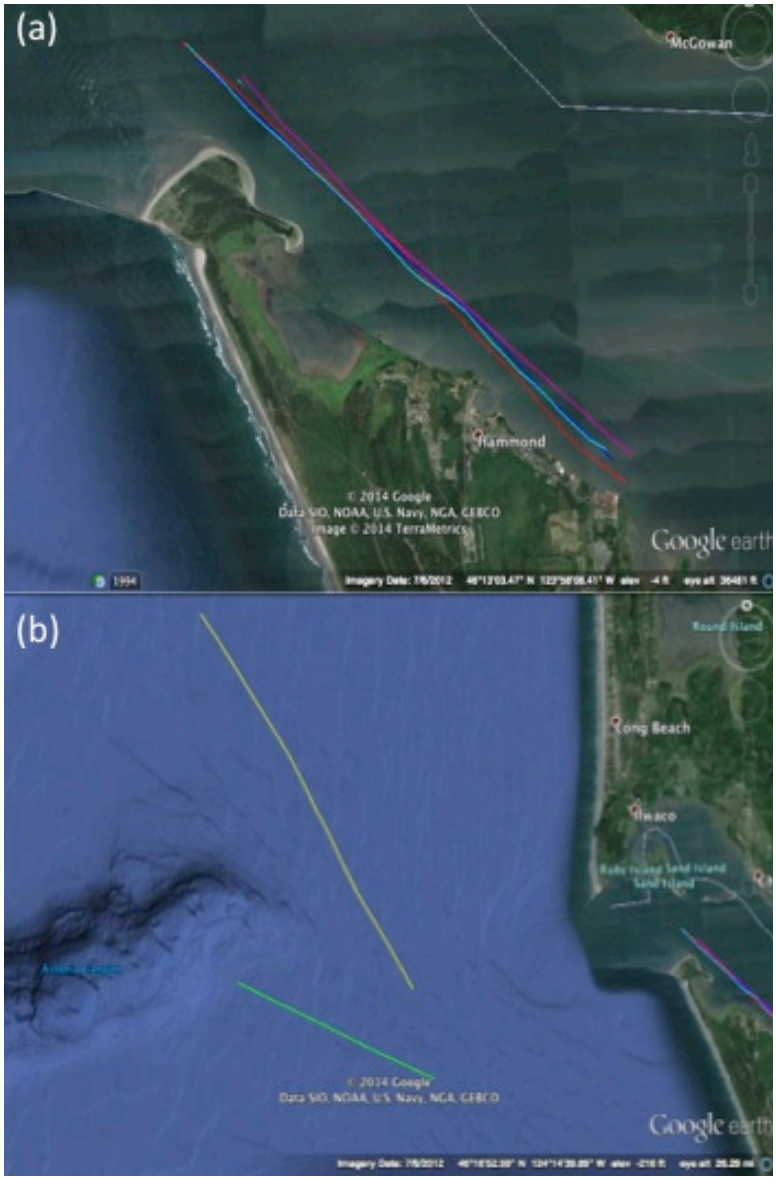

Figure 15. Final six transects. (a) Shows all six transects. (b) Shows four transects within the MCR. (c) Shows two transects outside the MCR close to the bar (after Google Earth 2014).

THIS PAGE INTENTIONALLY LEFT BLANK

V. FLOOD RESULTS

Data collection for the ADCP begins at a depth below the surface of 7.08 m due to ADCP blank range. This blank range serves multiple purposes by being a minimum distance necessary to avoid collecting bad data that has potentially been contaminated from ringing, and avoid flow noise from the bottom of the ship when hull-mounted (RD Instruments 2002).

Each transect observation and model vertical section are displayed for comparison along with transect start and end times, and NOAA predicted tidal current magnitudes and times. Each vertical section displays depth, longitude, and current speed and direction. Additionally, current vectors are plotted for selected depths to allow a more quantitative comparison of observation and model data. Transects will be divided for analysis by flood (Figure 16) and ebb (Figure 22).

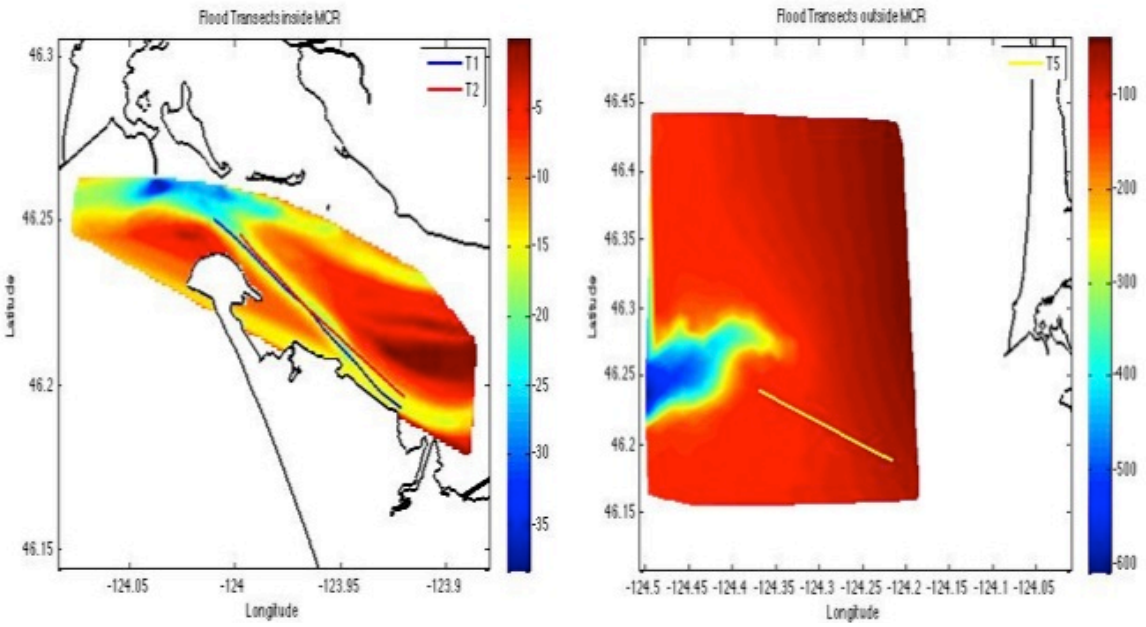

Figure 16. Transects during flood inside the MCR (left panel) and outside the MCR (right panel).

A. TRANSECT 1: PEAK FLOOD TO SLACK INSIDE MCR

Transect 1 was recorded on 06 Jun 2013 between 1946-2046 UTC. The ship was heading southeast upriver and peak flood was predicted to occur at 1838 UTC with slack predicted to occur at 2114 UTC. New moon occurred on 08 Jun just two days after, indicating this transect was very close to a neap to spring transition.

Observational data (Figure 17) shows that the current is directed upriver from the uppermost bin (7.08 m below the surface) throughout the remainder of the column. The effects of the bottom boundary layer are evident in the current weakening with depth towards the bottom. Stronger currents at the beginning of the period drastically weakened from 86 cm/s to approximately 20 cm/s in the middle of the period. Tidal current strength unexpectedly increased toward the end of approaching slack, predicted to occur just 28 minutes after the end of the transect.

SELFE model data shows a somewhat different picture. The strongest currents were predicted to be at the start of the period, as with the observational data, and the observed and predicted initial current speeds are in good agreement. As the period progressed toward slack water the model shows currents weakening throughout the column and even changing direction at the surface before the end of the period, indicating the development of an ebbing current at the surface while the lower water column is still flooding. While this phenomenon is well established, it could not be verified with the ADCP data, which do not cover the upper seven meters of the water column. Towards the end of the transect the model predicts notably weaker currents near the bottom than observational data.

A closer comparison of this data using current vector plots (Figure 18) at 7.08 m and 13.08 m for both sets of data shows differences as well. At 7.08 m, the observed current at the beginning of the period has a strong eastern component before gradually turning south and heading upriver. The current maintains this southern flow until -123.94° longitude; in the vicinity of the trench identified in Figure 10. It is possible that this trench is topographically steering the current back to an eastern direction of flow. Model data at 7.08 m shows a predominantly southern current along the entire transect.

The model data shows the current weaken much more toward the end of the period than does the observational data.

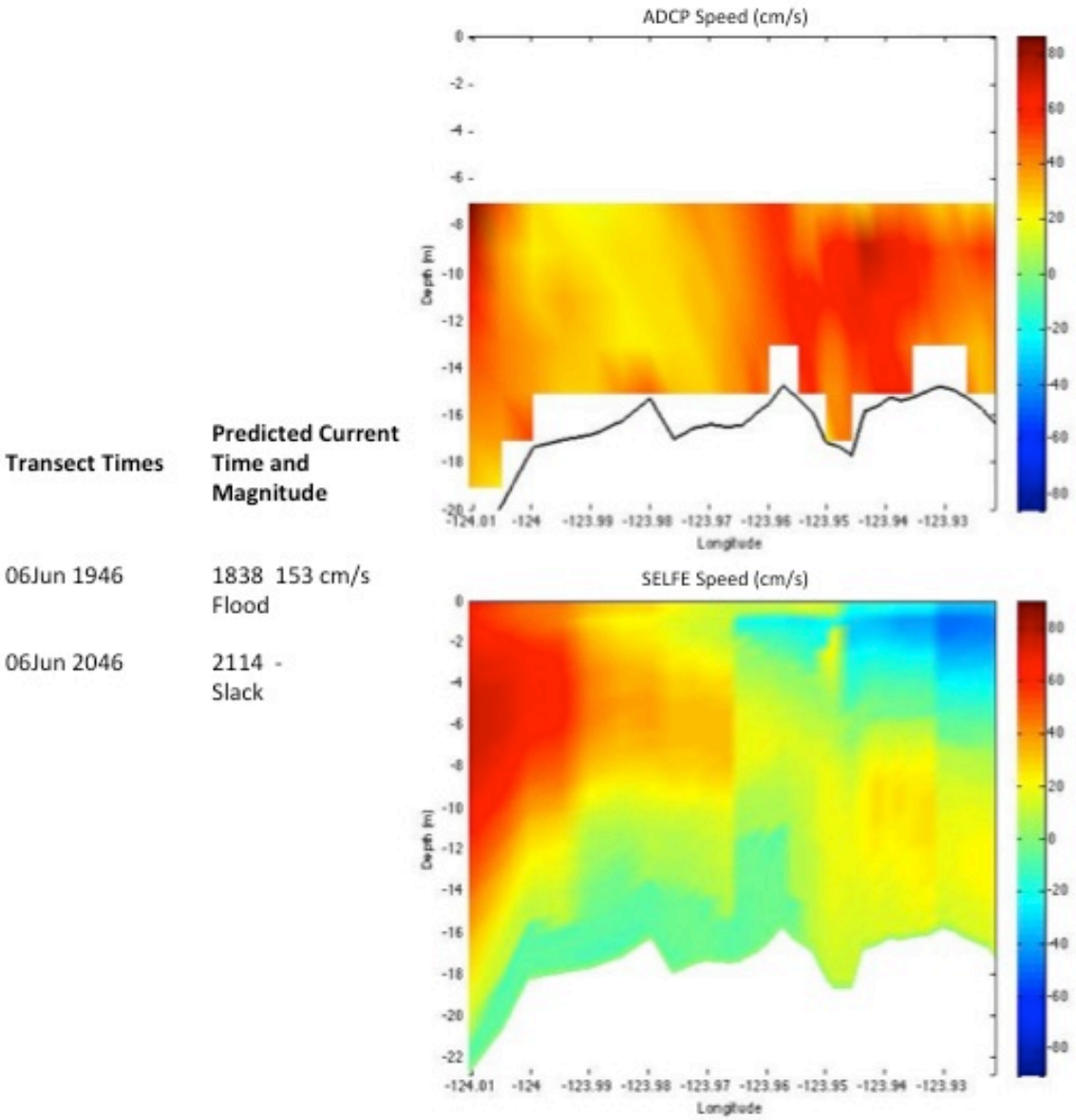

Figure 17. Transect 1 vertical section plots for ADCP (top panel) and SELFE (bottom panel) data. Current speed is shown in color with positive values indicating up-river (flood) flow and negative values indicating down-river (ebb) flow. NOAA predictions of max flood current and times of max flood and slack water at Clatsop Spit station are indicated on the left.

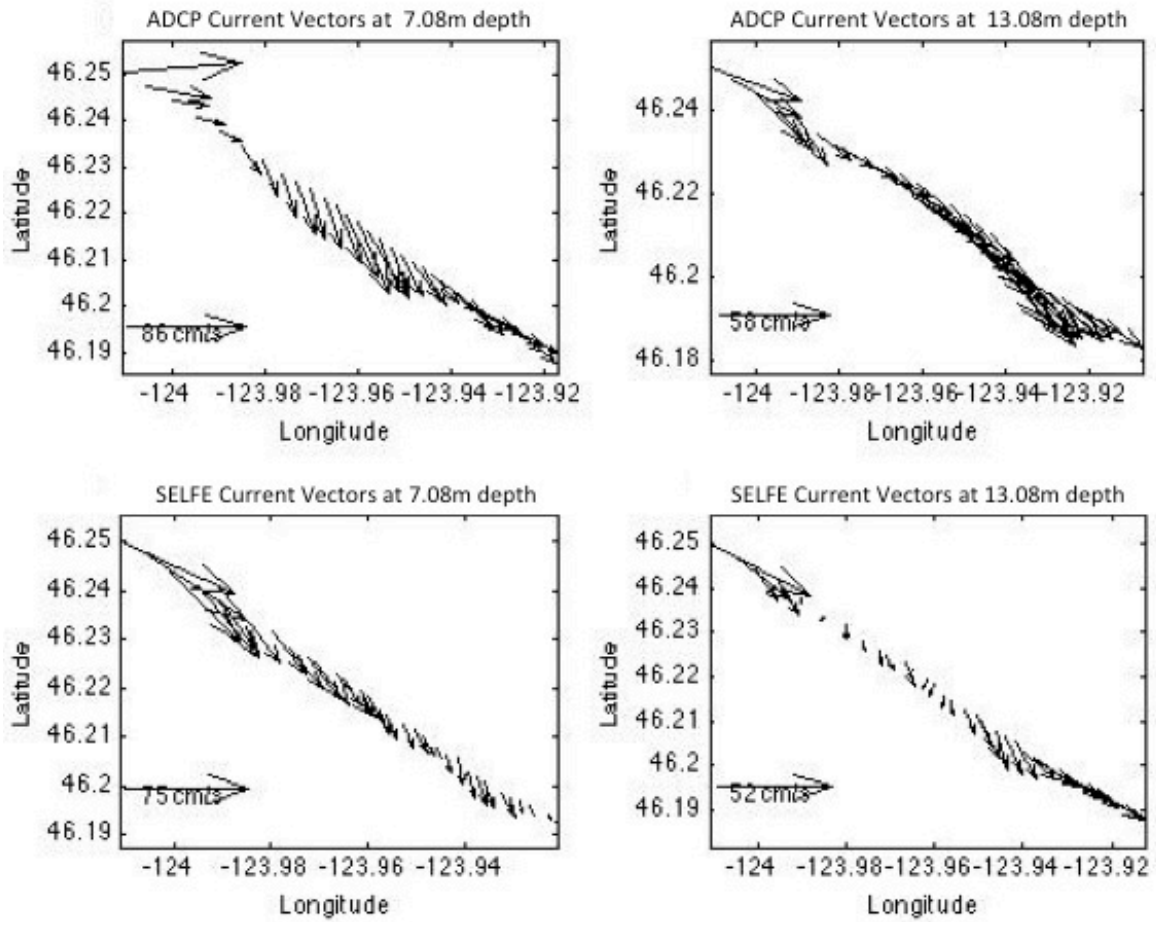

Figure 18. Transect 1 current vectors for ADCP (top panels) and SELFE (bottom panels) data at 7.08 m (left panels) and 13.08 m (right panels) depth.

B. TRANSECT 2: SLACK TO PEAK FLOOD INSIDE MCR

Transect 2 was recorded on 02 Jun 2013 between 1340-1424 UTC. The ship was heading northwest out to sea and slack was predicted to occur at 1145 UTC with peak flood predicted to occur at 1508 UTC. Third quarter moon occurred on 31 May, indicating this transect was recorded during a neap cycle.

ADCP vertical section plots (Figure 19) show weaker currents at the beginning of the transect after the passage of predicted slack water. The strongest currents occur in a region in the center of the transect that eventually begin to weaken as the transect period approaches predicted peak flood, which was predicted to occur 44 minutes after the end

of the transect. Again, this was an unexpected result. Assuming the predicted tidal current times to be accurate, it is reasonable to assume the tidal currents should begin to increase, especially considering how close the end of the transect is to peak flood. Instead the observation data shows peak flood occurring in the middle of the transect period and by the end is already transitioning to slack again. At 14 m the tidal currents begin to approach zero and even shift direction to flow out of the river. Prior to this, however, the currents strength is increasing with depth.

SELFE predictions agree with the ADCP observed weaker currents at the beginning of the transect period and the region of strong current in the center of the transect. Model data, however, does show stronger currents toward the end of the period as the transect approaches predicted peak flood. SELFE's use of a tide model that depends on predicted tides itself could be a possible explanation for this difference. The model data and observational data also disagree at the bottom boundary. The model does not show the current approaching zero as quickly as the observational data does. The model data also does not show current reversal at the bottom.

Further examinations into this transect using current vector plots (Figure 20) reveals good agreement among the observations and model with regards to direction and magnitude of the current throughout the water column. At 13.08 m both observations and model show a sudden southward shift in the current direction in the vicinity of the previously discussed trench. Again, this appears to be topographic steering occurring because of the trench, but more importantly, the model clearly predicts this behavior. The observational data shows a clear reversal at the end of the transect period at 13.08 m that is not predicted by the model.

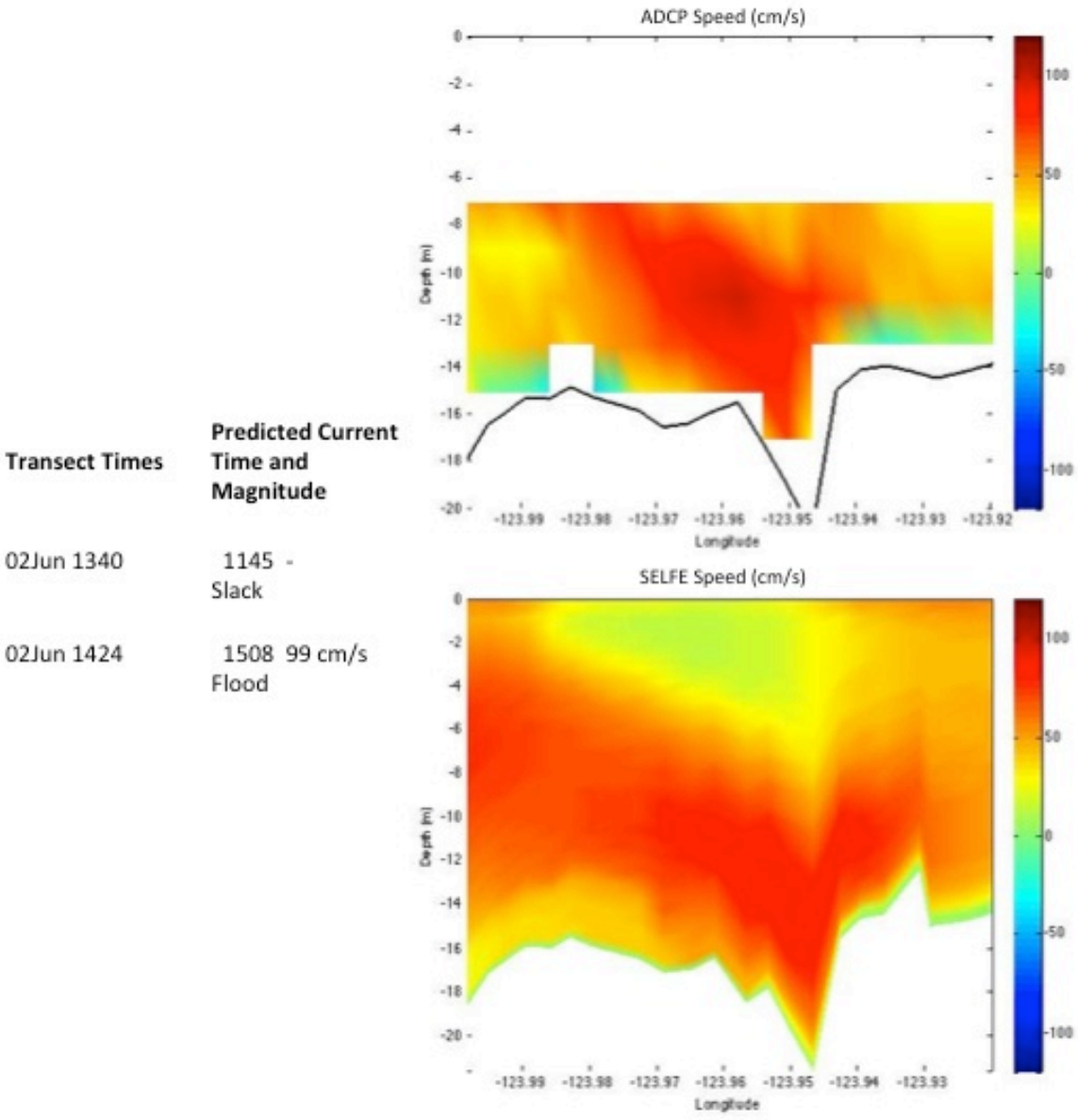

Figure 19. Transect 2 vertical section plots for ADCP (top panel) and SELFE (bottom panel) data. Current speed is shown in color with positive values indicating up-river (flood) flow and negative values indicating down-river (ebb) flow. NOAA predictions of max flood current and times of max flood and slack water at Clatsop Spit station are indicated on the left.

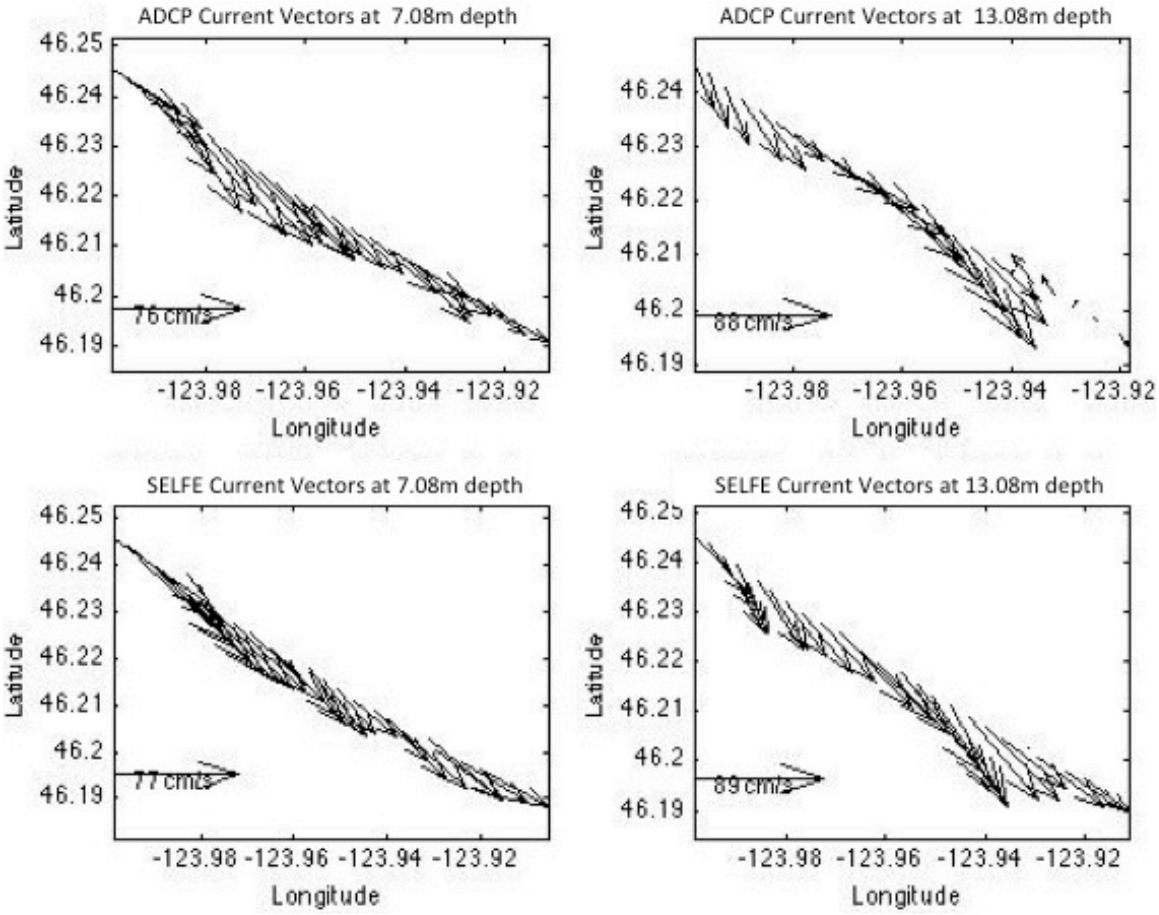

Figure 20. Transect 2 current vectors for ADCP (top panels) and SELFE (bottom panels) data at 7.08 m (left panels) and 13.08 m (right panels) depth.

C. TRANSECT 5: FLOOD OUTSIDE OF MCR

Transect 5 was recorded on 03 Jun 2013 between 0124-0214 UTC. The ship was heading southeast toward the river mouth and slack was predicted to occur at 02 Jun 2013 2315 UTC with peak flood predicted to occur at 0314 UTC. Third quarter moon occurred on 31 May indicating this transect was recorded during a neap cycle.

Vertical sections (Figure 21) for this transect were produced for both the *u* and *v* components of velocity. Vertical sections for the *u* component of velocity show a mild shoreward current throughout the column with weak seaward flow near the bottom. Vertical sections for the *v* component of velocity show a weak southern current

throughout the region with some intensification near the bottom in the middle of the transect.

Model data for both components of velocity shows homogeneous currents throughout the water column, with the exception of the upper few meters, and do not depict any the vertical structure with flow reversals that observations reveal. The models inability to define structure outside of the MCR is because the MCR SELFE model grid is tuned to focus on the estuary. The model grid outside of the estuary is coarser, which negatively affects accuracy. This region also lacks the substantial observational network that the estuary possesses (Karna 2014).

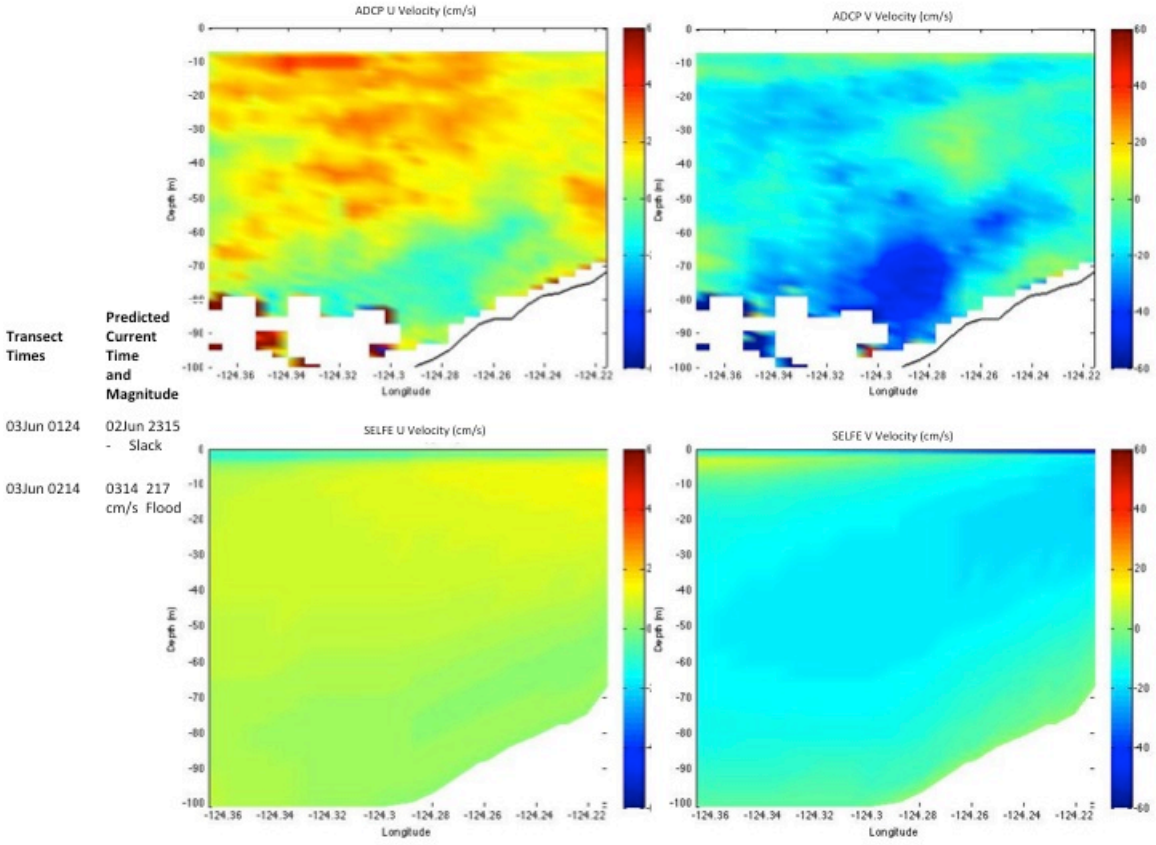

Figure 21. Transect 5 vertical section plots for ADCP observations (upper panels) and SELFE predictions (lower panels). Left panels: u component (+ eastward, - westward). Right panels: v component (+ northward, - southward)

VI. EBB RESULTS

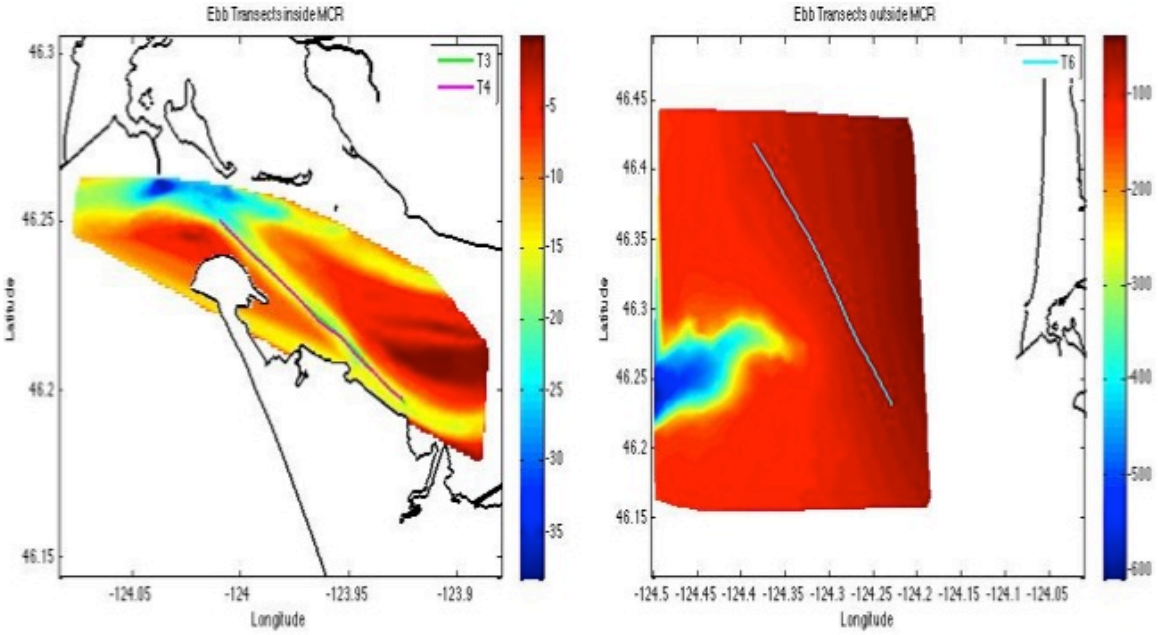

Figure 22. Transects on the left represent ebb data inside the MCR while the transect on the right represents ebb data outside of the MCR.

A. TRANSECT 3: PEAK EBB TO SLACK INSIDE THE MCR

Transect 3 was recorded on 09 Jun 2013 between 0240-0320 UTC. The ship was heading southeast upriver and peak ebb was predicted to occur at 0050 UTC with slack predicted to occur at 0351 UTC. New moon occurred on 08 Jun, indicating this transect was recorded during a spring cycle.

Slack water was predicted to occur 31 minutes after the end of the transect, preceding the transition back to flood. ADCP vertical section (Figure 23) plots show the flood current already forming at the beginning of the transect period. Strong ebb currents remain in the upper part of the water column and continue to ebb throughout the transect period. At 10 m the current strength approaches zero and begins to flood around 13 m. This is an interesting result because not only is the flood transition occurring well before the predicted times, but the strong flood currents near the bottom while the surface waters are still ebbing indicates there is no slack at all.

SELFE model predictions agree with the overall structure and timing of these events, but with some disparity in magnitude. Model data also shows the current continuing to ebb over the entire water column with weak flows, indicating a boundary layer near the bottom. The model also shows a period of time at the end of the transect in which the entire column approaches slack water. Weak upriver currents are predicted at the bottom, but overall the model is showing a transition to slack water.

Further analysis using current vectors (Figure 24) shows good agreement between the observations and the model at 7.08 m. Both observations and model prediction data show an ebbing current throughout the period at this depth, although the observational data shows a stronger current. Observations and model predictions differ greatly at 13.08 m. Observational data shows the current transitioning into a strong flood current at approximately a third of the distance of the transect. Model data shows the current weakening and approaching zero, and transitioning into a much weaker flood current towards the end of the period. Again, the model current vectors at this depth resemble a transition to slack water, whereas the observational data at this depth clearly show a transition to flood current.

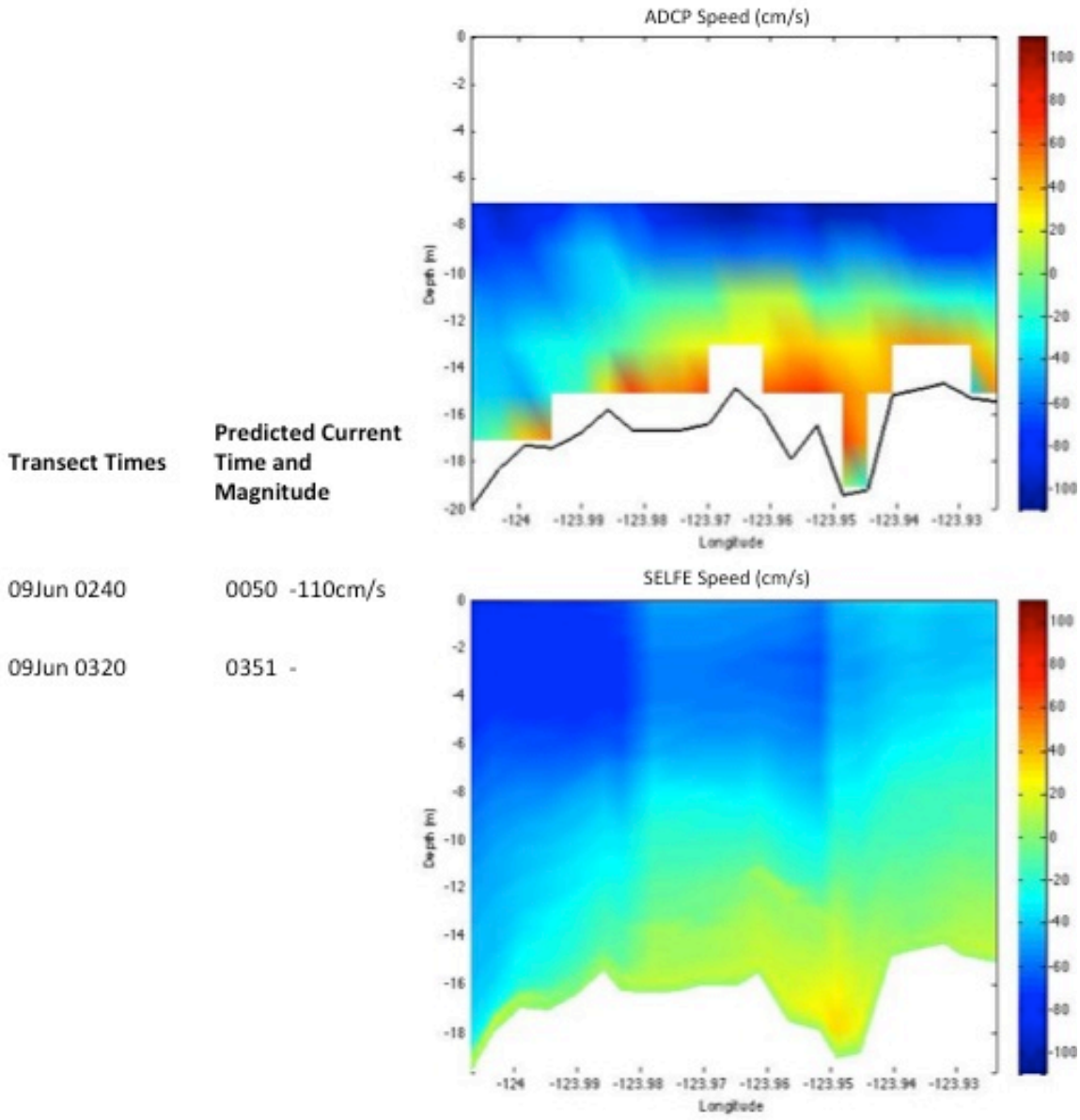

Figure 23. Transect 3 vertical section plots for ADCP (top panel) and SELFE (bottom panel) data. Current speed is shown in color with positive values indicating up-river (flood) flow and negative values indicating down-river (ebb) flow. NOAA predictions of max ebb current and times of max ebb and slack water at Clatsop Spit station are indicated on the left.

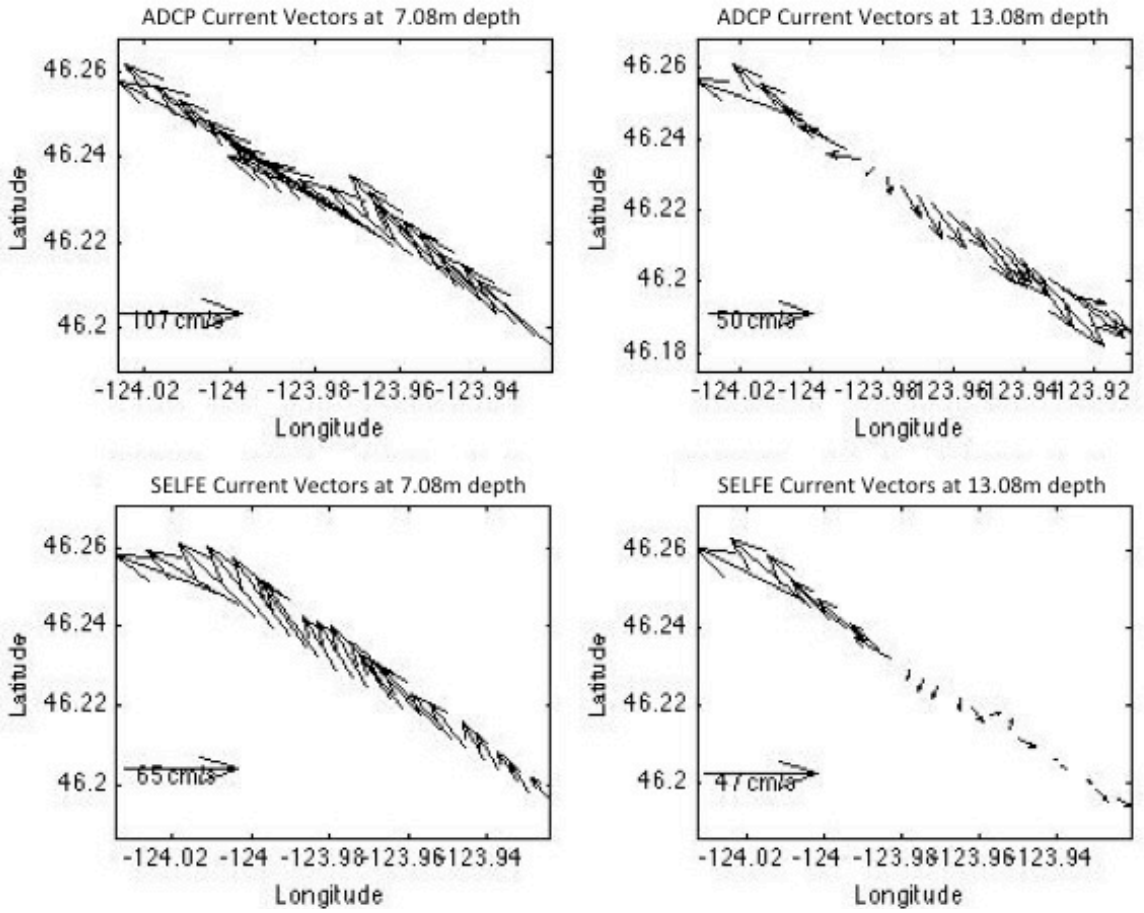

Figure 24. Transect 2 current vectors for ADCP (top panels) and SELFE (bottom panels) data at 7.08 m (left panels) and 13.08 m (right panels) depth.

B. TRANSECT 4: SLACK TO PEAK EBB INSIDE THE MCR

Transect 4 was recorded on 30 May 2013 between 1458-1558 UTC. The ship was heading southeast upriver and slack was predicted to occur at 1344 UTC with peak ebb predicted to occur at 1644 UTC. Third quarter moon occurred on 31 May, just one day after the recording of this data, indicating this transect was transitioning from spring to neap cycle.

ADCP vertical sections (Figure 25) show a strong (2 m/s) ebb current, with a maximum at the upper most bin (7.08 m) and much weaker currents near the bottom. As

the transect progresses the stronger currents extend further down the column, and by the end the period a strong well-defined ebb current is observed at all depths.

SELFE model predictions are in excellent agreement with the observational data. There is a strong ebb current throughout the column with weaker currents in the center of the transect near the bottom. The region of weakening current is smaller in the model data, but is represented in the same location. Observed and predicted current strength agree well.

Further analysis using current vectors (Figure 26) shows good agreement between observations and model predictions At 13.08 m depth, observed and predicted current direction show the current slightly veering to the north around the vicinity of the trench identified within the main navigation channel. This shift to north vice south during flood is consistent with a topographic steering effect. Overall, observed and predicted vertical current structures are in excellent agreement on this transect.

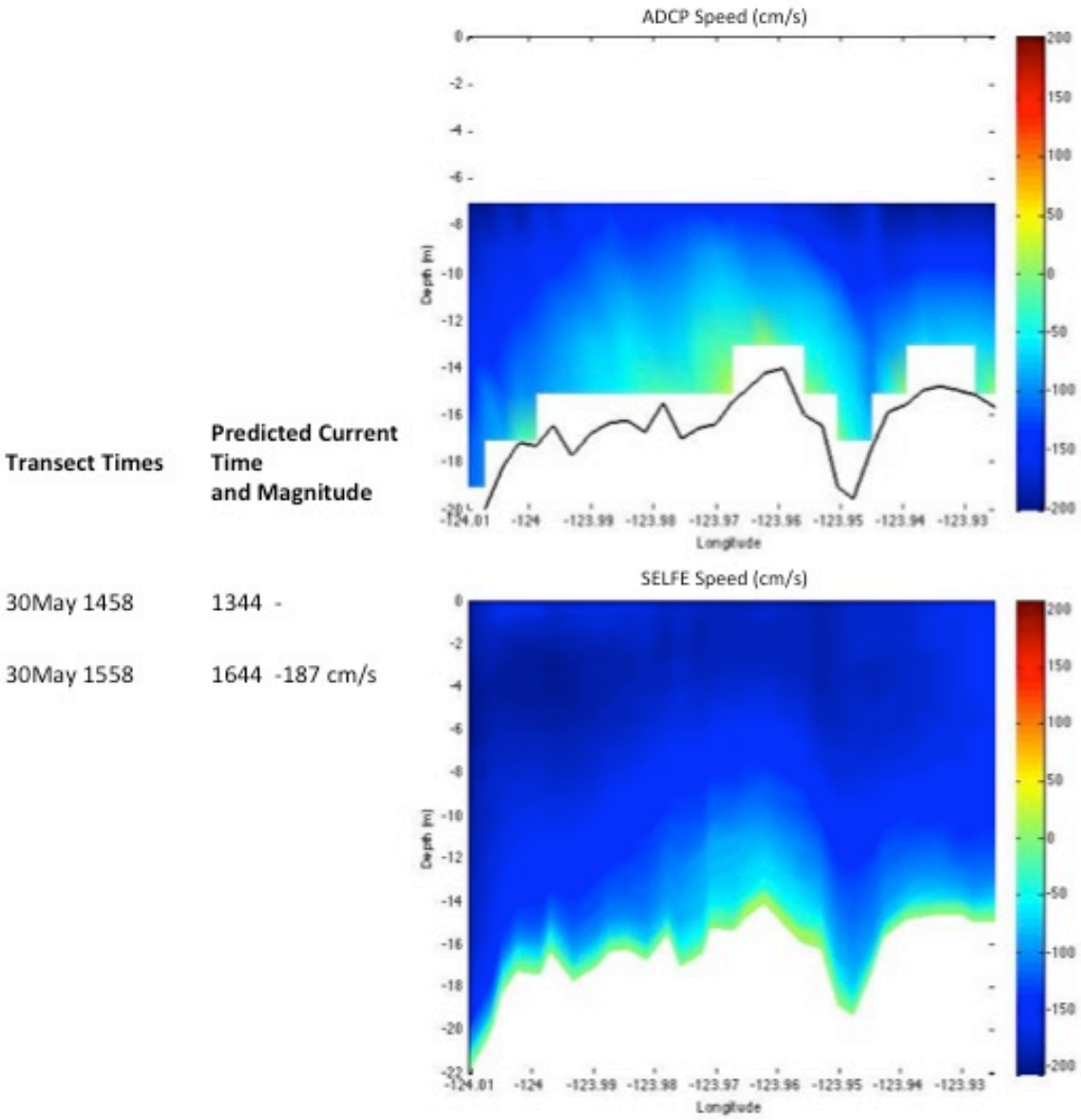

Figure 25. Transect 4 vertical section plots for ADCP (top panel) and SELFE (bottom panel) data. Current speed is shown in color with positive values indicating up-river (flood) flow and negative values indicating down-river (ebb) flow. NOAA predictions of max ebb current and times of max ebb and slack water at Clatsop Spit station are indicated on the left.

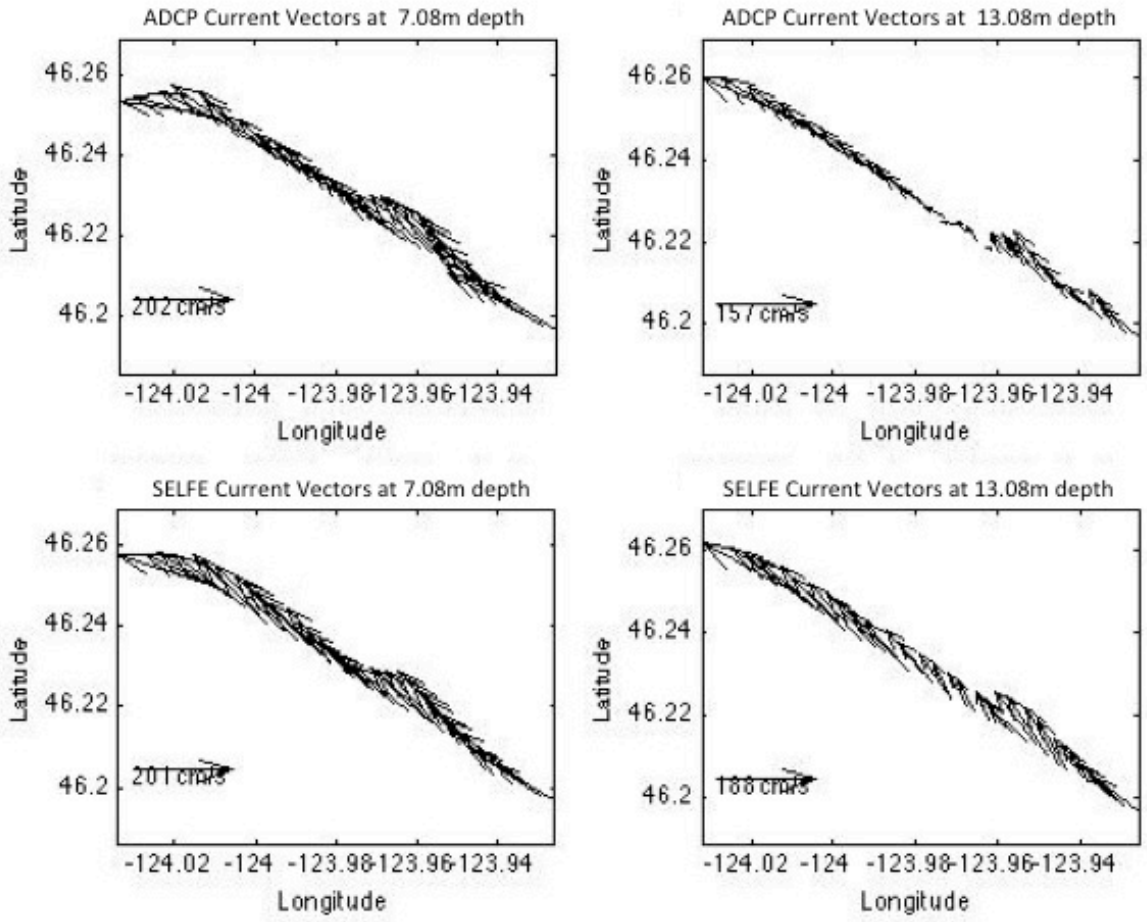

Figure 26. Transect 4 current vectors for ADCP (top panels) and SELFE (bottom panels) data at 7.08 m (left panels) and 13.08 m (right panels) depth.

C. TRANSECT 6: EBB OUTSIDE OF MCR

Transect 6 was recorded on 31 May 2013 between 1900-2048 UTC. The ship was heading southeast toward the river mouth and peak ebb was predicted to occur at 1750 UTC with slack predicted to occur at 2121 UTC. Third quarter moon occurred on 31 May indicating this transect was recorded during a neap cycle.

Vertical sections (Figure 28) for this transect were produced for both the *u* and *v* components of velocity. Vertical sections for the *u* component of velocity show a weak seaward current on the surface with a stronger shoreward current in the bottom 20 m. Vertical sections for the *v* component of velocity show a strong northward current in the

top 20 m the plot. Below this depth the current weakens and turns to flow southward along the bottom.

Model predictions show relatively homogeneous conditions throughout the column and stronger current in the upper 10 m of the water column. The model does show a strong ebb current near the surface in the second half of the transect (negative u, positive v) in qualitative agreement with observations but the detailed vertical structure looks rather different.

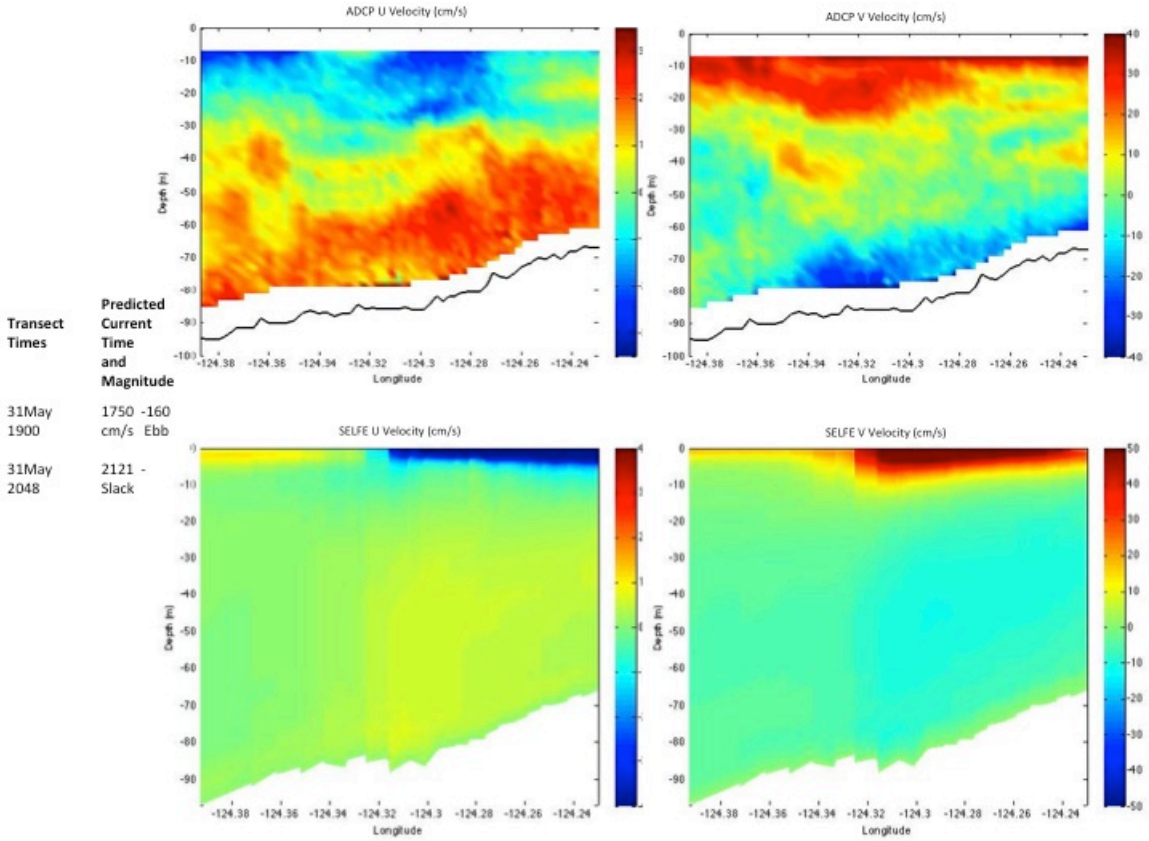

Figure 27. Transect 6 vertical section plots for ADCP observations (upper panels) and SELFE predictions (lower panels). Left panels: u component (+ eastward, - westward). Right panels: v component (+ northward, - southward)

VII. CONCLUSION

A. SUMMARY

1. MCR Shipboard ADCP Measurements

The vertical tide structure of the MCR is not well understood, in large part, due to a lack of sufficient measurements. The objectives of this research were to characterize the vertical structure of the tidal within the MCR over various tidal cycles, and validate the SELFE model's ability to predict these currents.

To investigate the vertical structure of the tidal currents, ADCP measurements collected during a three-week long cruise within the MCR were broken up into transects. This was accomplished by extracting periods of data collected while traversing the main navigation channel and the bar region at a relatively constant speed and heading. The initial three-week data set was reduced to 16 transects: 11 inside the river and five outside the river, seaward of the river mouth. A subset of these transects are presented here that characterize the vertical structure at different tidal stages.

2. Observed Vertical Structure

Early in the flood cycle the vertical structure exhibits two-layer flow with a strong flood current along the bottom and a slight river outflow on the surface. As the period approaches peak flood, the entire water column experiences a complete reversal in flow to a flood current. This complete reversal in flow through the entire water column can be seen as far upriver as the Astoria-Megler Bridge.

The ebb current is more homogenous throughout the water column than the flood current. River outflow acts in unison with the ebb current to produce a stronger current. During higher range tidal periods slack water is often bypassed altogether, with a flood current developing in the lower part of the water column while strong ebb flows continue in the surface layer. This sudden transition from one strong tidal cycle to the next with no slack water in between is one of the many dangers mariners face when navigating the channel.

3. SELFE Model Evaluation

The SELFE model is an operational flow model developed and run by the Oregon Health and Science University. The SELFE model solves the shallow-water equations on an unstructured grid, which allows the resolution to vary within a single model domain. The model solves its primary variables in three dimensions. Model inputs come from observation stations within the river, meteorological databases, and oceanographic forcing models.

Inside the river, the SELFE model performed qualitatively well in comparison to the observations. The model showed good agreement for nine out of the original 11 transects inside the river, whereas Transects 1 and 3, showed significant differences between model and observations. The data from these two transects were collected during periods approaching slack. In the transition from flood to slack the predictions show weaker currents in the lower part of the water column than is observed, whereas in the transition from ebb to slack the predicted reversal to a near-bottom flood current is weaker than is observed.

Outside of the river the SELFE model does not resolve the detailed vertical structure of the observed currents. This is not surprising as the grid resolution outside of the mouth is coarser than the grid resolution inside the mouth. The area of the model domain outside of the mouth of the river also suffers from limited observational inputs whereas the estuary has a well-established observational network to which the model is calibrated.

B. FUTURE RESEARCH

The ADCP is becoming a standard instrument included in many ships' inventories. Collecting ADCP data while vessels transit through coastal and tidal inlets could help shed light on the vertical structure and wave-current interactions occurring in these dynamic regions. These observations are useful in the immediate evaluation of local area models and dynamics. Collecting these observations and storing them in a database can also allow them to be used in the future for characterizing the dynamics in specific regions around the world.

The development of an automated analysis scheme could make the collection and evaluation of these data simpler for mariners who do not possess the knowledge and expertise required to manage these data. This would allow the data to be collected by a crew, stored during their cruise, and delivered upon return to port to a central location for automated analysis and archiving.

The ADCP observations collected during this experiment do not provide information in the top 7 m of the water column, thus excluding comparison of surface observations with the model surface predictions. Surface drifter data, however, were also collected in the experiment (Pearman 2014). Analysis of the combined ADCP and drifter data will allow for a more complete analysis of the vertical structure of the tidal currents in the MCR.

THIS PAGE INTENTIONALLY LEFT BLANK

LIST OF REFERENCES

Bowditch, N., 2002: *The American Practical Navigator.* 2002 Bicentennial Edition. National Imagery and Mapping Agency, 882 pp.

Burla, M., A. M. Baptista, Y. Zhang, and S Frolov, 2010a: Seasonal and internannual variability of the Columbia River plume: A perspective enabled by multiyear simulation databases. *J. Geophys. Res.,* **115**, 1-25, doi:10.1029/2008JC00.4964

Burla, M., A. M. Baptista, E. Casillas, J. G. Williams, and D. M. Marsh, 2010b: The influence of the Columbia River plume on the survival of steelhead (Oncorhynchus mykiss) and Chinook salmon (Oncorhynchus tshawytscha): a numerical exploration. *Can. J. Fish. Aquat. Sci.,* **67**, 1671-1684, 10.1139/F10-083.

CMOP, cited 2014: Columbia River Estuary. [http://www.stccmop.org/news/2013/cmop_study_provide_insight_biogeochemical_exchange_between_bays_estuary]

Disney, L. P., and W. H. Overshiner, 1925: *Tides and Currents in San Francisco Bay.* Department of Commerce, 123 pp.

Elias, E. P. L., G. Gelfenbaum, and A. J. Van der Westhuysen, 2012: Validation of a coupled wave-flow model in a high-energy setting: The mouth of the Columbia River. *J. Geophys. Res*, **117**, n/a–n/a, doi:10.1029/2012JC008105.

Google Inc., 2013: Google Earth 7.1.2.2041. Google.

Gonzales, F. I., 2000: A Case Study of Wave-Current-Bathymetry Interactions at the Columbia River Entrance. *J. Phys. Oceanogr.*, **14**, 1065–1078.

Gross, M. G., and E. Gross, 2005: *Online Ocean Studies.* American Meteorological Society, 404 pp.

Jay, D.A., and J. D. Smith, 1990: Circulation, density distribution and neap-spring transitions in the Columbia River Estuary. *Prog. Oceano.*, **25**, 81-112.

Jay, D. A., K. Leffler, and S. Degens, 2011: Long-Term Evolution of Columbia River Tides. *J. Waterway, Port, Coastal, Ocean Eng*, **137**, 182–191, doi:10.1061/(ASCE)WW.1943-5460.0000082.

Jay, D. A., C. A. Simenstad, D. C. McIntire, W. Nehlsen, and C. R. Sherwood, 1984: The Dynamics of the Columbia River Estuarine Ecosystem: Volume I and Volume II, CREDDP. *Civil and Environmental Engineering Faculty Publication and Presentations*, **1**, 1–363.

Karna, T., Oregon Health & Science University Institute of Environmental Health, 2014, personal communication.

Kilcher, L. F., and J. D. Nash, 2010: Structure and dynamics of the Columbia River tidal plume front. *J. Geophys. Res*, **115**, C05S90, doi:10.1029/2009JC006066.

Koch, M., and H. Sun, 1999: Tidal and non-tidal characteristics of water levels and flow in the Apalachicola Bay, Florida. *Coastal Engineering & Marina Development,* Brebbia, C. A., and Anagnostopoulos P., WIT Press, 357-366.

Lutz, G. A., D. W. Hubbell, and H. H. Stevens Jr, 1975: *Discharge and flow distribution, Columbia River estuary. Transport of radio nuclides by streams*. United States Department of Interior

MetEd COMET Program, cited 2014: Introduction to Ocean Currents. [http://www.meted.ucar.edu/oceans/currents/print.htm - 3.2]

Meyer, E. P., A. M. Baptista, 2001: Inversion for tides in the Eastern North Pacific *Ocean. Adv. Water Resour.,* **24**, 505-519.

NOAA Tides, cited 2014: NOAA Predicted and Observed Tides. [http://tidesandcurrents.noaa.gov/noaatidepredictions/NOAATidesFacade.jsp?Stationid=9439011

NOAA Observed Water Levels, cited 2014: NOAA Hammond Station Observed Water Levels. http://tidesandcurrents.noaa.gov/waterlevels.html?id=9439011&units=metric&bdate=20130525&edate=20130615&timezone=GMT&datum=MLLW&interval=6&action=%5D]

Pearman, D. W., 2014: Wave Evolution in River Mouths and Tidal Inlets. Naval Postgraduate School, 105 pp.

Physical Oceanography Department, WHOI. (n.d.). Ocean Instruments: ADCP. Retrieved from Woods Hole Oceanographic Institution website: http://www.whoi.edu/page.do?pid=8415&tid=3622&cid=819

Portell, J. R., 2013: Calibration and Validation of Inertial Measurement Unit for Wave Resolving Drifters. Graduate School of Engineering and Applied Sciences, Naval Postgraduate School, 83 pp.

RD Instruments, 1996: *Acoustic Doppler Current Profilers Principles of Operation: A Practical Primer.* 2nd ed. RD Instruments, 54pp.

RD Instruments, 2002: *Workhorse Acoustic Doppler Current Profiler Technical Manual.* RD Instruments Acoustic Doppler Solutions, 196 pp.

Shchepetkin, A.F., J. C. McWilliams, 2005. The regional oceanic modeling system (ROMS): a split-explicit, free-surface, topography-following-coordinate, oceanic model. *Ocean Model*. **9**, 347–404, doi:10.1016/j.ocemod.2004.08.002.

Simenstad, C. A., D. A. Jay, D. C. McIntire, and L. F. Small, 2002: Columbia River Estuary studies: An introduction to the estuary, a brief history, and prior studies. *Prog. Oceano.*, **25**, 1–13.

Simpson, M. R., 2001: *Discharge Measurements Using a Broad-Band Acoustic Doppler Current Profiler.* U. S. Department of Interior, 123 pp.

Strong, B., B. Brumley, E. A. Terray, and G. W. Stone, 2000: The performance of ADCP-derived directional wave spectra and comparison with other independent measurements. *OCEANS 2000 MTS/IEEE Conference and Exhibition,* 2, Providence, RI, IEEE, 1195-1203.

Teledyne RD Instruments, cited 2014: Workhorse Mariner 1200, 600, 300 kHz ADCP. [http://marineops.mlml.calstate.edu/sites/default/files/wh_mariner_ds_lr.pdf]

Templeton, W. J., and D. A. Jay, 2013: Lower Columbia River Sand Supply and Removal: Estimates of Two Sand Budget Components. *J. Waterway, Port, Coastal, Ocean Eng*, **139**, 383–392, doi:10.1061/(ASCE)WW.1943-5460.0000188.

Turner, P., Oregon Health & Science University-CMOP, 2014, personal communication.

Umlauf, L., H. Burchard, 2003. A generic length-scale equation for geophysical turbulence models. *J. Mar. Res.*, **61**, 235–265, doi:10.1357/002224003322005087.

Wewetzer, S. F. K., R. W. Duck, and J. M. Anderson, 1999: Acoustic Doppler current profiler measurements in coastal and estuarine environments: example from the Tay Estuary, Scotland. *Geomorphology,* **29,** 21-30.

Wikipedia, cited 2014: Columbia River Mouth and Bar. [http://commons.wikimedia.org/wiki/File:Columbia_River_Mouth_and_Bar.jpg])

THIS PAGE INTENTIONALLY LEFT BLANK

INITIAL DISTRIBUTION LIST

1. Defense Technical Information Center
   Ft. Belvoir, Virginia

2. Dudley Knox Library
   Naval Postgraduate School
   Monterey, California